Doctoral Dissertations and Master's Theses

Fall 12-2015

Lagrangian Points and Jacobi Constants for a Class of Asteroids

Tasneem Rashid
Embry-Riddle Aeronautical University

LAGRANGIAN POINTS AND JACOBI CONSTANTS

FOR A CLASS OF ASTEROIDS

A Thesis

Submitted to the Faculty

of

Embry-Riddle Aeronautical University

by

Tasneem Rashid

In Partial Fulfillment of the

Requirements for the Degree

of

Master of Science in Aerospace Engineering

December 2015

Embry-Riddle Aeronautical University

Daytona Beach, Florida

LAGRANGIAN POINTS AND JACOBI CONSTANTS
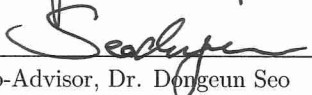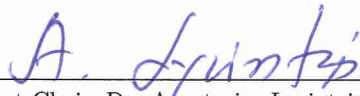# FOR A CLASS OF ASTEROIDS

by

Tasneem Rashid

A Thesis prepared under the direction of the candidate's committee chairman, Dr. Yechiel Crispin, Department of Aerospace Engineering, and has been approved by the members of the thesis committee. It was submitted to the School of Graduate Studies and Research and was accepted in partial fulfillment of the requirements for the degree of Master of Science in Aerospace Engineering.
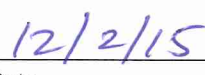
THESIS COMMITTEE
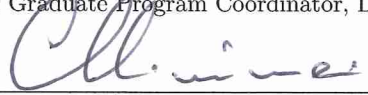
_____ 12/2/2015
Chairman, Dr. Yechiel Crispin

_____ 12/2/2015
Co-Advisor, Dr. Dongeun Seo

_____ 12/2/2015
Member, Dr. Mahmut Reyhanoglu

_____
Department Chair, Dr. Anastasios Lyrintzis
or Graduate Program Coordinator, Dr. Eric Perrell

12/2/15
Date

_____
Dean of College of Engineering, Dr. Maj Mirmirani

12/3/15
Date

_____
Associate VP for Academics, Dr. Christopher Grant

12/3/15
Date

ACKNOWLEDGMENTS

TABLE OF CONTENTS

LIST OF TABLES

LIST OF FIGURES

SYMBOLS

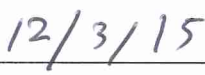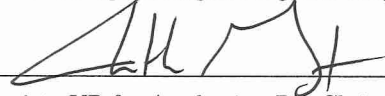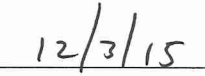|	
a_{rel}	Relative acceleration of spacecraft relative to the rotating frame of reference
a,b,c	Semi-principal axes of an ellipsoid respectively
C	Jacobi Integral
C_{lm}, S_{lm}	Gravity field Harmonic Co-efficients
G	Gravitational constant
Ln	n^{th} Lagrangian Point
μ	Standard Gravitational parameter
m_n	Mass of nth body
Ω	Angular velocity
Ω_c	Characteristic Angular velocity
$P_{lm}(x)$	Associated Legendre Function
r_{lm}	Distance between centers of spheres l and m
r_n	Position vector of nth body
r_o	Characteristic/ Normalizing radius of a body
ρ_n	Density of nth body
σ_n	Mass ratio of nth body
t	Time
T	Time period
t_c	Characteristic Time
T_c	Characteristic Time period
U_n	Gravitational Potential of nth body
v	Speed of spacecraft relative to the rotating frame of reference
v_{rel}	Relative velocity of spacecraft relative to the rotating frame of reference

ABSTRACT

Rashid, Tasneem MSAE, Embry-Riddle Aeronautical University, December 2015. La-

grangian Points and Jacobi Constants for a Class of Asteroids.

Asteroid Gravitational Potentials are difficult to model owing to their irregular-
ity in shape. This thesis focuses on two approaches to model asteroid gravity fields,
namely, multiple-body and spherical harmonics modeling. Computation of gravity
potential serves as a first step to determine equilibrium points called Lagrangian
points for a spacecraft orbiting an asteroid. Further, Jacobi analysis is carried out
to determine zero-velocity regions, i.e., inaccessible regions corresponding to the un-
stable Lagrangian points. Multiple sphere modeling was studied through analysis of
so called Asteroid Restricted Three and Four Body Problems, providing insight into
the method of modeling an asteroid as a cluster of multiple spheres in contact with
each other and rotating with a constant angular velocity about the center of mass of
the cluster. A spherical harmonics approximation was then investigated for a special
case, an asteroid in the shape of an ellipsoid. This approach is common but yields
highly complex equations of motion due to multiple terms in the spherical harmon-
ics expansion. Finally the equivalence of the above two methods was validated by
considering a configuration of a cluster of spheres that can approximate an ellipsoid.

1. INTRODUCTION

1.1 Formation of Asteroids

The solar nebula hypothesis, proposed by Kant and Laplace, explains the formation of our solar system. The solar system developed from a gigantic cloud of gas and dust. This cloud was composed of highly dispersed material. Gravity caused this scattered mass to come together. As the masses were attracted to the core of the nebula, its gravity increased exponentially attracting more material. This led to friction, radiating heat and culminating in nuclear fission reactions, giving birth to the center of our solar system - the Sun. Meanwhile, the rest of the mass formed a scattered disc orbiting the Sun. These materials started coming together as planetesimals, owing to gravity. Those nearer the sun were composed of metal and rock while those farther away cooled to ice and gas clouds. Some of these planetesimals built up to the eight planets we know today - Mercury, Venus, Earth, Mars, Jupiter, Saturn, Uranus and Neptune. The formation of planets facilitated the sweeping up of the scattered materials around the Sun.

However, beyond the orbit of Mars, the formation of a planet was hindered by immense gravity of the largest planet Jupiter. Hence there exists a belt of dispersed planetesimals between the orbits of Mars and Jupiter. These planetesimals are termed Asteroids and this belt is called the Main Asteroid belt. The main belt has around

0.7-1.7 million asteroids, and their combined mass would yet be just half of the mass of Earth's moon. Many of them have moons too. Four of the largest asteroids are Ceres, Vesta, Pallas and Hygiea. The asteroids are classified into C-type i.e. carbonaceous, S-type i.e., silicate and M-type i.e., metallic asteroids, based on their composition. Ceres was the first asteroid to be discovered while Gaspra was the first asteroid to be approached by a space mission Galileo in 1991.

The asteroids constantly collide with each other and this also contributes to the absence of a planet in the main belt. Also, the swing effect of Jupiter's gravity causes some of the largest asteroids to be ejected from the main belt into the inner solar system or into the Kuiper belt. The Kuiper belt is a trans-Neptunian asteroid belt where the asteroids are mostly composed of ice. The asteroids which have been flung into the inner solar system by the swing effect of Jupiter's gravity, either collide with planets or collapse into the sun. Some of these have come near the Earth and are hence termed Near Earth Asteroids (NEA). Studying these Asteroids may uncover a lot of information about the solar system and also prevention of collisions of asteroids with the Earth.

1.2   Near Earth Asteroids

The asteroids in the vicinity of the Earth's orbit are called Near Earth Asteroids (NEA). The semi-major axis of their orbits, is less than 1.3AU from the Sun. There are more than 10,000 NEAs with dimensions ranging from 1m - 32km. The largest NEA is Ganymed and is $34.28km \times 31.66km$ in dimension. It was discovered by Walter

Baade in 1924. The NEAs are classified into four categories based on the distance of their orbits from the sun. They are Atiras, Atens, Apollos and Amors. The Atiras asteroids have orbits strictly within the Earth's orbit. The Atens asteroids have semi-major axis less than 1AU from the sun but aphelion distance greater than 0.983 AU which means they cross Earth's orbit, while Apollos asteroids have semi-major axis greater than 1AU and cross Earth's orbit too. Finally, the Amors asteroids have orbits strictly outside that of Earth's and some of them cross the Martian orbit too. This classification enables us to determine Potentially Hazardous Asteroids (PHA) which may threaten to impact the Earth. An asteroid falls under the PHA category when it approaches closer than 0.05AU of an Earth Minimum Orbit Insertion Distance (MOID), and has an absolute magnitude less than 22m i.e., it cannot get closer to the Earth than 0.05AU and diameter greater than 150m. The largest PHA known currently is Toutalis. There are 1592 PHAs known as of now.

The NEAs are part of a larger group called The Near Earth Object (NEO) group. This consists of meteoroids, and comets in addition to asteroids. These pose hazards to the Earth too. As of February 2014 around 11000 NEOs have been discovered. Hence study of these objects is important to protect and prevent damage to the Earth due to collisions.

1.3   Asteroid Missions

Asteroids are composed of materials which are the building blocks of planets. Hence asteroid missions reveal important information regarding the origin of our so-

lar system. Moreover, some asteroids, for example Pallas and Hygiea have organic compounds and previously had water. Further, their current chemical composition is similar to the primeval solar system. This would allow us to study the origin of life on Earth. Asteroids harbor valuable metals which can be mined and studied. Mining fragments from asteroid may give us a chance to study the solar system during different eras. Another important reason for asteroid missions is that scientists are now considering trying to modify an asteroid's trajectory by deflecting it. This in addition to an asteroid collision threat provide sufficient reasons for asteroid exploration mission.

There have already been a couple of asteroid missions in the past. The first space mission to closely approach an asteroid in terms of a flyby was the Galileo mission in 1991 which captured images of Gaspra and Ida. It also imaged Ida's moon Dactyl. This marked the beginning of asteroid missions. This was followed by several missions like the Cassini, NEAR Shoemaker, Rosetta, Hayabusa etc. These missions have enabled scientists to infer important information about our solar system. For example Pluto, which was initially considered the ninth planet has been demoted to the status of a minor planet. Ceres, the largest asteroid has been now termed a dwarf planet too owing to its size and mass. These missions are designed to capture images of asteroids and to orbit them, attempt landings and send back material and data to the Earth ground stations, and further get into the orbits of Mars and Jupiter as a secondary part of their mission. Rosetta has successfully landed its lander module Philae on comet 67P. This probe will now orbit the comet nucleus and move with

it alongside on its journey towards the sun. This would be the ultimate mission to understand the life cycle of a comet, its formation and decay. Hayabusa, a JAXA mission, was the first to return material from a Near Earth Asteroid- Itokawa. If not for its failed lander MINERVA, Hayabusa would have been the first asteroid hopper. Thus asteroid spin, trajectory, impact threat, formation, life span etc. can be understood through such missions.

Current missions now include the DAWN mission which is currently orbiting the largest asteroid-dwarf planet Ceres. This is the second asteroid it is orbiting since its journey along the second largest asteroid Vesta. Also the New Horizons space probe is set to explore the most prominent member of the Kuiper belt Pluto. It is scheduled to make its closest approach of Pluto on July 14 2015.The Hayabusa 2 an asteroid sample return mission, is en route to Near Earth asteroid 1999 JU3. It is a successor of Hayabusa but advanced since it plans to dig up the asteroid surface and retrieve fresh sample material.

Future missions include the OSIRIS-REx which is scheduled to launch on September 3 2016. This is again an asteroid sample return mission, with Bennu as its target asteroid. The objective of this mission is to document the asteroid's surface, collect data as well as enough sample to study asteroid formation, the Yarkovsky effect and future impact threats as well as potential resources in asteroids. Another very bold mission proposed by NASA is the Asteroid Redirect mission. Sample return missions are expensive, extend for years and carry great risk especially in the deployment of landers. This mission intends to grab a boulder from an asteroid and insert in a stable

lunar orbit, so astronauts may access it easily and in a very short span. Not only this, bringing back a huge sample, may burn it during reentry to the Earth. This way the sample becomes much more easily accessible.

1.4   Asteroid Modeling - Background Literature

Since asteroids are highly irregularly shaped, their gravitational potentials are not simple to compute. Planets, on the contrary, are spheroids (slightly oblate spheres) and hence have approximately uniform gravity fields. Computation of gravitational potential plays an important role in determination of equilibrium positions, called Lagrangian points and further estimate the Jacobi regions (forbidden regions i.e., inaccessible for navigation of a spacecraft), corresponding to these Lagrangian points. Several approaches have been proposed to overcome the complexities of modeling the gravity fields of irregularly shaped of asteroids (E. Herrera Sucarrat & Roberts, 2013). They are discussed below.

Spherical harmonics: This is one of the most commonly used technique (Scheeres, 2012). It is basically a solution of the Laplace equation. It employs a number of harmonic co-efficients to mimic the potential function on an irregular surface. This approach however is a series expansion. Hence, truncation leads to loss of accuracy. In addition, the nature of the terms becomes increasingly complex at higher orders and this, increases the computation time and cost. Also this approximation assumes the irregular body to have uniform mass distribution. Hence, the series diverges when

the proximity to the asteroid increases. This approximation will be discussed in detail in Chapter 4.

Polyhedron model: This model also assumes the asteroid under consideration to be of uniform and constant density (Werner, 1993). It approximates the asteroid as a polygon with multiple planar faces to approximate its surface features like craters and ridges, as accurately as possible. It suffers from the same divergence issues as Spherical Harmonics due to the constant density assumption.

Mascon model: The *Mascon* or *Mass concentration model* (Werner & Scheeres, 1996) computes the gravitational potential by approximating the asteroid as a uniform three dimensional mesh with point masses at the vertices of the grid points. These point masses may of equal or unequal densities and the sum total of the point masses is matched to be the same as that of the asteroid. For example, the asteroid *Castalia* was filled with 3300 point masses to approximate the mass and mass distribution of the actual asteroid. This method accounts for mass distribution but this approach is asteroid specific as it requires a lot of data regarding the geometry, shape and density variation. Hence it cannot be applied for a general case.

Another approach discussed in detail in this thesis, is multiple body modeling. This approach provides a simple method of determining the gravitational potential by approximating an irregular body by a number of constant and equal density spheres or other symmetric shapes, for example an ellipsoid. The advantage of this approach is that, the gravity potentials of symmetric shapes like spheres are closed form solutions and simpler to determine than the tedious harmonics approach.

To get further insight into multiple body modeling, Asteroid Restricted Three body problems are studied as a first step. Restricted three body and Restricted Full Three Body Problems (RF3BP) (i.e. both primaries rotating with different angular speeds), an extension of full two body problems, have been well documented by Werner and Scheeres. However, the above problems considered, do not investigate the case where the primaries are in contact with each other and rotate with a constant angular speed. This is an important point to be considered when modeling a single asteroid as a multiple sphere system, since the masses are expected to be in contact with each other. Figure 1.1 shows asteroid *Itokawa* as an asteroid which can be split into lobes of different densities.

Figure 1.1. Asteroid Itokawa (Nermiroff & Bonnell, 2014)

D. J. Scheeres (Scheeres, 2012) has extensively studied the modeling of asteroids using spherical harmonics, and determination of gravity potentials, Langrangian
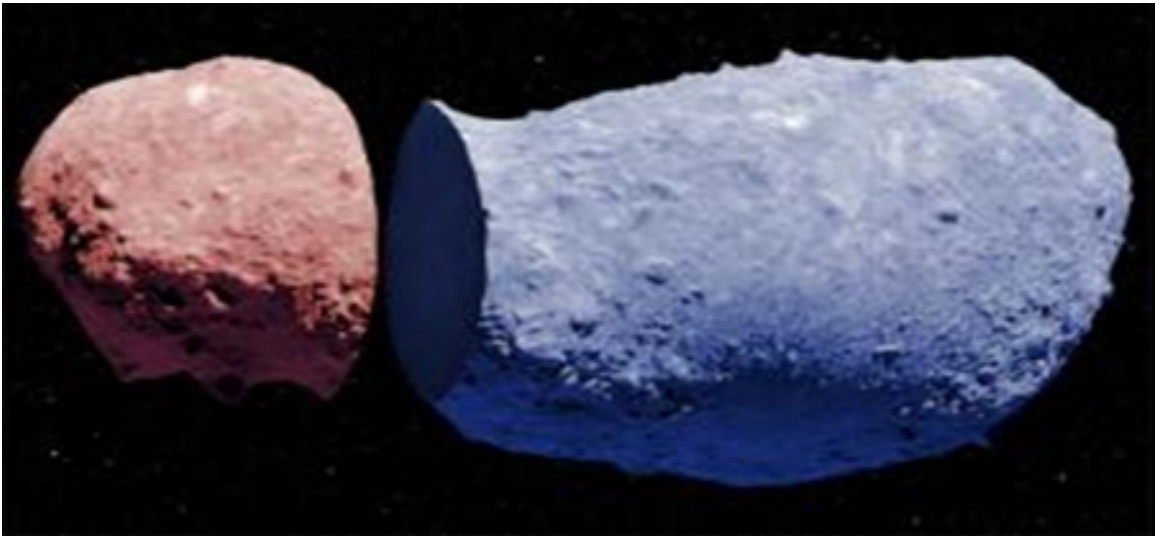
Figure 1.2. Asteroid Itokawa represented as two lobes of different densities (Lowry, 2014)

points and Jacobi regions. Complete analysis of the asteroid *Betulia* (C. Magri, 2007) provides a good understanding of the order of expansion of the harmonic approximation to compute the gravity potential and to find the Lagrangian points. Further, Scheeres has also documented the application of spherical harmonics to model the gravity potential of an ellipsoid. All the above literature has laid the background for correlating the two problems - modeling of asteroids using multi body modeling instead of spherical harmonics and as a special case of validation, an ellipsoid is modeled as three spheres of varying masses and their equilibrium points are compared.

1.5   The Problem Statement

The major objective of this thesis is the application of multiple-body modeling for computation of gravitation potential of asteroids. Further, equilibrium points and Jacobi integrals are evaluated using the above approach. The underlying motive is to replace the spherical harmonics modeling approach which is highly complex and computationally demanding, by multiple sphere modeling by the comparison of their respective equilibrium positions.

1.6   Organization of the Thesis

The first part of the thesis *(Chapter 2)* discusses the Restricted Three Body Problem. An extension to this case is applied by analyzing the Restricted Four Body Problem *(Chapter 3)*. Multiple configurations of the primaries are considered in both

cases. Further an ellipsoid is modeled using spherical harmonics *(Chapter 4)*. Finally the multiple-body modeling approach is validated by comparison of Lagrangian points yielded by an ellipsoid modeled as a cluster of three spheres, by spherical harmonics and that modeled by multi-sphere modeling approach *(Chapter 5)*.

2. THE ASTEROID RESTRICTED THREE BODY PROBLEM

2.1 Introduction

The three-body problem is a classical problem in orbital mechanics, to analyze the motion of three bodies, based on their data at a particular time, specifying their masses, velocities and positions. This traditionally came into existence in Isaac Newtons *Principia*. Prior to the invention of the chronometer - a device to determine the longitude at sea, one of the approaches was to use the position of the moon as guidance. But as its motion about the Earth was perturbed due to the gravity of the Sun, the problem gained importance and was addressed by Amerigo Vespucci and Galileo Galilei. The most common three body problems are those concerning the Sun-Earth-Moon system or Earth-Moon-Spacecraft system.

Bruns and Poincare have shown that there is no general analytical solution for the three body problem. Hence, some restrictions were imposed which generated the concept of a *Restricted Three Body Problem*. These restrictions impose that one of the three bodies has a negligible mass and gravity with respect to the other two. This negligible mass is referred to as the secondary body and the other two, as primary bodies. This secondary mass orbits the primaries in an x-y plane, with respect to the center of mass of the primary mass system. The primaries in general have a large mass difference and are separated by huge distances (E.g. Earth-Moon-Spacecraft System).

In our multiple-body modeling approach, the analysis of this Restricted Three Body Problem plays an important role. This is because another important restriction is imposed on the above problem in addition to the existing assumptions. The primaries are considered to have relatively comparable masses and are brought in contact with each other such that they rotate with a constant angular velocity together about their common center of mass. This helps to mimic a binary asteroid system at the simplest case. Addition of further masses to this system provides further insight into the multi-sphere modeling approach.

Let us consider a system of two spheres (primaries) of equal and constant density, rigidly connected to each other and rotating with a constant angular velocity, $\Omega \hat{k}$. The spheres may (symmetric case) or may not (asymmetric case) be of equal masses. A spacecraft (secondary mass) orbits the above sphere system in an x-y plane. Let r be the position vector of the spacecraft with respect to the center of mass O of the sphere system. Similarly r_1 and r_2 are the position vectors of the spacecraft with respect the centers mass of spheres *1* and *2* respectively. The co-ordinate axes are fixed to the sphere system, in the rotating frame of reference, such that, the origin is at the O. The spheres have a circular orbit about O. The following diagram depicts the above mentioned system.
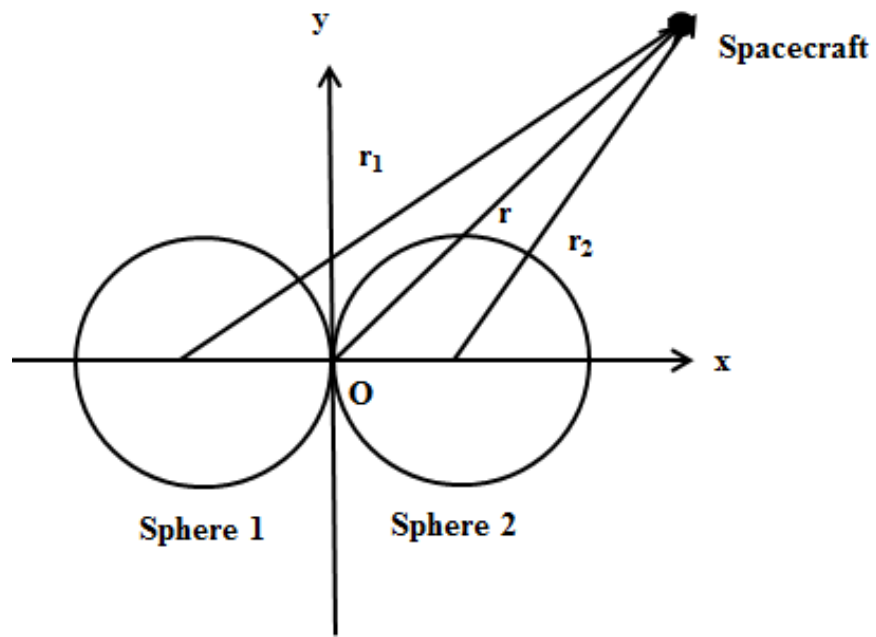
Figure 2.1. Symmetric sphere system
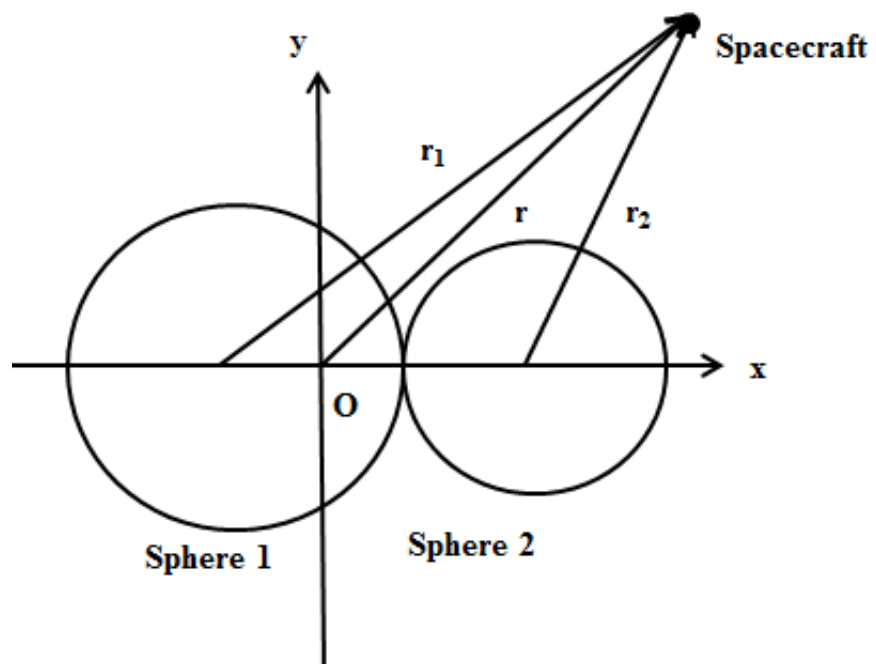
Figure 2.2. Asymmetric sphere system

2.2   Gravitational Potential

Estimation of the Gravity Potential is the first step to obtain the equations of motion, followed by the determination of Lagrangian points and Jacobi Analysis. The gravitational potential of a sphere is expressed as follows.(Curtis, 2010)

$$U = \frac{\mu}{r} \tag{2.1}$$

where,

$\mu = Gm =$ Gravitational constant of the sphere, km^3/s^2

$r =$ position vector of the spacecraft with respect to center of mass of the sphere, km

Let r_{12} be the distance between the centers of the two spheres. Let m_1 and m_2 be their respective masses and, σ_1 and σ_2 be their respective mass ratios. The position vectors mentioned earlier can now be defined as follows. The terms in the *x-components* are different due to spread of the spheres along the *x-axis*.

$$m_1 + m_1 = m \tag{2.2}$$

$$\mu_1 = Gm_1; \mu_2 = Gm_2 \tag{2.3}$$

$$\sigma_1 = \frac{m_1}{m_1 + m_2}; \sigma_2 = \frac{m_2}{m_1 + m_2} \tag{2.4}$$

$$r^2 = x^2 + y^2 + z^2 \tag{2.5}$$

$$r_1^2 = (x + \sigma_2 r_{12})^2 + y^2 + z^2 \tag{2.6}$$

$$r_2^2 = (x - \sigma_1 r_{12})^2 + y^2 + z^2 \tag{2.7}$$

Thus, the gravitational potential due to each individual sphere is given as follows,

$$U_1 = \frac{\mu_1}{r_1}; U_1 = \frac{\mu_2}{r_2} \tag{2.8}$$

Hence, the total gravitational potential due to both the spheres is,

$$U = U_1 + U_2 \tag{2.9}$$

2.3 Equations of Motion

Once the gravity potential has been determined, the equations of motion can be derived from Newton's second law as follows. It is to be noted that the total acceleration $\ddot{r}$ is in the inertial frame of reference.

$$m\ddot{r} = F \tag{2.10}$$

where, $F = \nabla U$

Let v_{rel} and a_{rel} be the relative velocity and acceleration with respect to the rotating frame of reference, respectively. The general acceleration formula, accounting for Coriolis force and centripetal acceleration is as follows,

$$\ddot{r} = \Omega \times (\Omega \times r) + 2\Omega \times v_{rel} + a_{rel} \tag{2.11}$$

where,

$$v_{rel} = \dot{x}\hat{i} + \dot{y}\hat{j} + \dot{z}\hat{k} \tag{2.12}$$

$$a_{rel} = \ddot{x}\hat{i} + \ddot{y}\hat{j} + \ddot{z}\hat{k} \tag{2.13}$$

From the above definitions, the equations of motion in the x, y and z directions respectively can be framed as given below.

$$\ddot{x} - 2\Omega\dot{y} - \Omega^2 x = \frac{\partial U}{\partial x} \tag{2.14}$$

$$\ddot{y} + 2\Omega\dot{x} - \Omega^2 y = \frac{\partial U}{\partial y} \tag{2.15}$$

$$\ddot{z} = \frac{\partial U}{\partial z} \tag{2.16}$$

The derivatives are then computed to get the following final equations of motion,

$$\ddot{x} - 2\Omega\dot{y} - \Omega^2 x = -\frac{\mu_1}{r_1^3}(x + \sigma_2 r_{12}) - \frac{\mu_2}{r_2^3}(x - \sigma_1 r_{12}) \tag{2.17}$$

$$\ddot{y} + 2\Omega\dot{x} - \Omega^2 y = -\frac{\mu_1}{r_1^3}y - \frac{\mu_2}{r_2^3}y \tag{2.18}$$

$$\ddot{z} = -\frac{\mu_1}{r_1^3}z - \frac{\mu_2}{r_2^3}z \tag{2.19}$$

To analyze a general case, it is a good practice to non-dimensionalize the equations. Now, all distances are non-dimensionalized with respect to r_{12}. All parameter with the over-bar notation represent non-dimensionalized quantities.

$$x = \bar{x}r_{12}; y = \bar{y}r_{12}; z = \bar{z}r_{12}$$

$$r = \bar{r}r_{12}; r_1 = \bar{r_1}r_{12}; r_2 = \bar{r_2}r_{12}$$

The angular velocity, time and time period are non-dimensionalized with respect to their characteristic counterparts, Ω_c, t_c and T_c.

$$T_c = 2\pi\sqrt{\frac{r_{12}^3}{\mu}}$$

$$t_c = \sqrt{\frac{r_{12}^3}{\mu}}$$

$$\Omega_c = \sqrt{\frac{\mu}{r_{12}^3}}$$

Post non-dimensionalization, the equations transform as follows.

$$\ddot{\bar{x}} - 2\bar{\Omega}\dot{\bar{y}} - \bar{\Omega}^2\bar{x} = -\frac{\sigma_1}{\bar{r}_1^3}(\bar{x} + \sigma_2) - \frac{\sigma_2}{\bar{r}_2^3}(\bar{x} - \sigma_1) \tag{2.20}$$

$$\ddot{\bar{y}} + 2\bar{\Omega}\dot{\bar{x}} - \bar{\Omega}^2\bar{y} = -\frac{\sigma_1}{\bar{r}_1^3}\bar{y} - \frac{\sigma_2}{\bar{r}_2^3}\bar{y} \tag{2.21}$$

$$\ddot{\bar{z}} = -\frac{\sigma_1}{\bar{r}_1^3}\bar{z} - \frac{\sigma_2}{\bar{r}_2^3}\bar{z} \tag{2.22}$$

2.4 Lagrangian Points

In celestial mechanics, Lagrangian points are equilibrium positions of a small mass (spacecraft) in an orbital configuration of two larger masses, such that in the rotating frame, the smaller mass always appears to be stationary. There are five such points. L1, L2 and L3 lie on the line connecting the larger masses, while L4 and L5 each form an equilateral triangle with them. The equilateral triangle assumption holds good only when the system of primary masses does not rotate beyond its natural characteristic angular velocity Ω_c. The Lagrangian points L4 and L5 are determined first. At equilibrium positions, all time derivatives reduce to zero i.e.

$$\ddot{\bar{x}} = \ddot{\bar{y}} = \ddot{\bar{z}} = \dot{\bar{x}} = \dot{\bar{y}} = \dot{\bar{z}} = 0 \tag{2.23}$$

Hence, the system of non-dimensional equations reduces to the following.

$$\bar{\Omega}^2\bar{x} = -\frac{\sigma_1}{\bar{r}_1^3}(\bar{x} + \sigma_2) - \frac{\sigma_2}{\bar{r}_1^3}(\bar{x} - \sigma_1) \tag{2.24}$$

$$-\bar{\Omega}^2\bar{y} = -\frac{\sigma_1}{\bar{r}_1^3}\bar{y} - \frac{\sigma_2}{\bar{r}_1^3}\bar{y} \tag{2.25}$$

$$0 = -\frac{\sigma_1}{\bar{r}_1^3}\bar{z} - \frac{\sigma_2}{\bar{r}_1^3}\bar{z} \tag{2.26}$$

The above system yields the following analytical solutions.

$$\bar{x} = \frac{1}{2}(\sigma_1 - \sigma_2) \tag{2.27}$$

$$\bar{y} = \pm\sqrt{(\frac{1}{\bar{\Omega}})^{\frac{4}{3}} - \frac{1}{4}} \tag{2.28}$$

$$\bar{z} = 0 \tag{2.29}$$

An important conclusion can be drawn from the above results. It is to be noted that $\bar{x}$ is independent of $\bar{\Omega}$, while $\bar{y}$ is purely a function of $\bar{\Omega}$. From this a limiting value of $\bar{\Omega}$ can be obtained. This was found to be *2.8283* i.e., for $\bar{y} = 0$; $\bar{\Omega} = 2.8283$. The following graph shows the variation of the y-co-ordinate of L4 and L5 with respect to $\bar{\Omega}$

From Figure 2.3, it is observed that at $\bar{\Omega} = 0$, $\bar{y} \to \infty$. Physically this implies that, when $\bar{\Omega} = 0$, the primaries are not rotating and hence the centripetal acceleration tends to zero implying zero gravity. Hence the equilibrium position escapes to infinity. Conversely, when $\bar{\Omega} = 2.8283$ *(limiting condition)*, $\bar{y} \to 0$. This means that, when the primaries rotate beyond their maximum angular speeds, the centripetal acceleration becomes very high, implying a corresponding increase in the gravity field. This causes the equilibrium position to coalesce at the center of mass of the primary system.

The other Lagrangian points, L1, L2 and L3 are determined next. Since these points lie along the longitudinal axis i.e. x-axis of the system, $\bar{y}$ is set to zero,
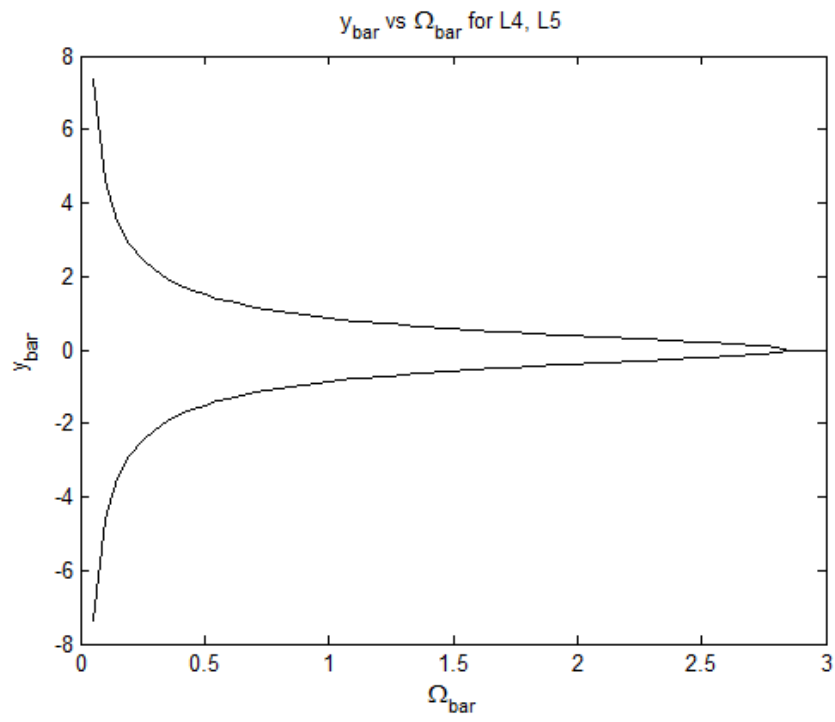
Figure 2.3. Plot of y-co-ordinates of L4 and L5 with respect to $\bar{\Omega}$

in addition to all the previous assumptions. Hence, we are left with the following equation which gives three roots (i.e. x-co-ordinates of L1, L2 and L3).

$$\frac{\sigma_1}{\bar{r}_1^3}(\bar{x} + \sigma_2) - \frac{\sigma_2}{\bar{r}_1^3}(\bar{x} - \sigma_1) - \bar{\Omega}^2\bar{x} = 0 \tag{2.30}$$

where,

$$\bar{r}_1 = |\bar{x} + \sigma_2|; \bar{r}_2 = |\bar{x} - \sigma_1|$$

The above equation is highly non-linear and hence cannot be solved analytically. It was thus solved numerically for different cases of $\bar{\Omega}$ as shown in the plots below. The plots are a function of the $\bar{x}$-co-ordinates of the L1, L2 and L3 with respect to the mass ratio of the sphere 2. L2 is a negative root while L3 is positive. L1 may be positive, zero or negative. A special case occurs for $\sigma_2 = 0.5$ (implying a symmetric case) where L1 = 0 and, L2 and L3 have equal magnitudes but opposite directions.

2.5 Jacobi Analysis

The Jacobi Analysis is carried out to determine the Jacobi Integral and also the Jacobi regions for a classical three body system. The Jacobi region envelopes the zero velocity curves and maps a *forbidden region* which cannot be crossed by a spacecraft. This plays an important role during the navigation of a spacecraft in close proximity to an asteroid. The prime objective of the Jacobi Analysis is to map permissible regions around the Lagrangian points L1, L2 and L3. This is because these points are
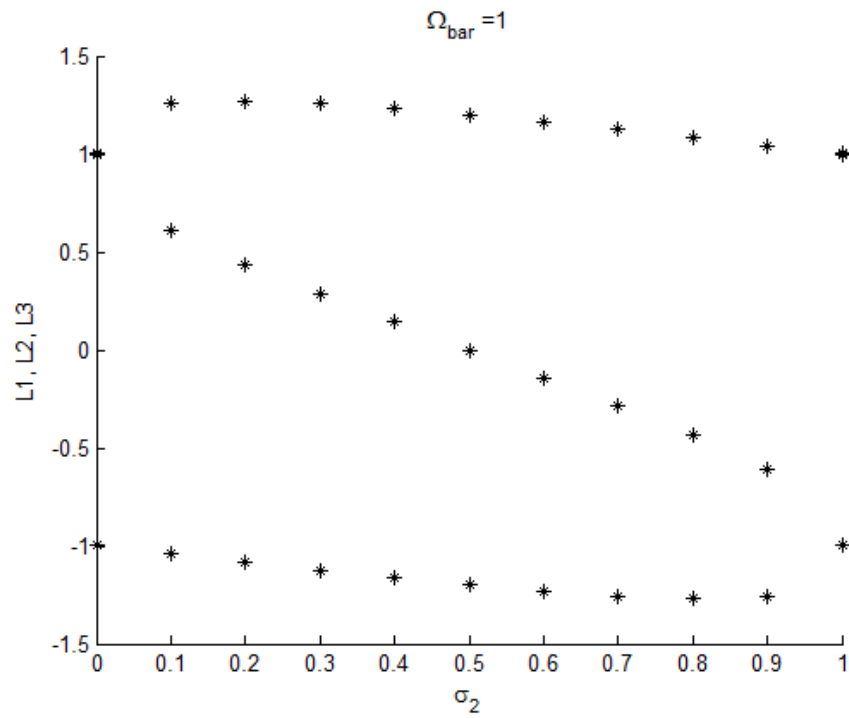
Figure 2.4. Plot of x-co-ordinates of L1, L2 and L3 with respect to σ_2 for $\bar{\Omega}=1$
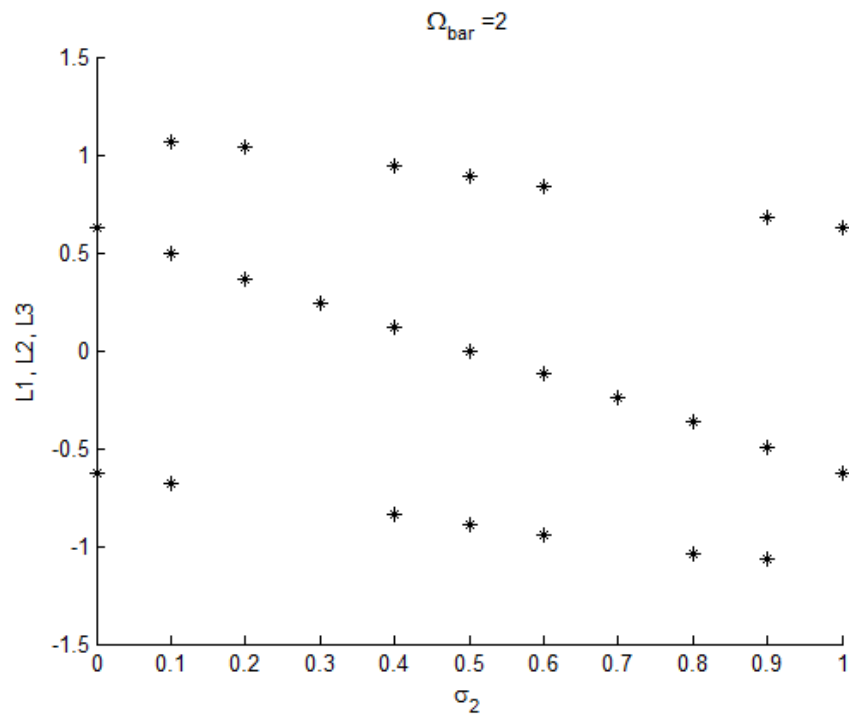
Figure 2.5. Plot of x-co-ordinates of L1, L2 and L3 with respect to σ_2 for $\bar{\Omega}=2$
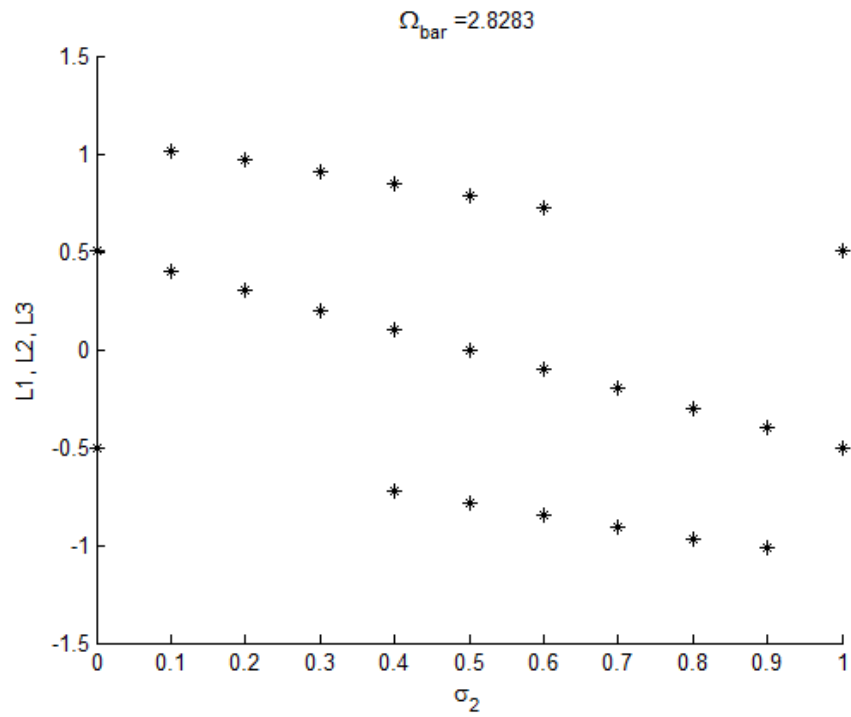
Figure 2.6. Plot of x-co-ordinates of L1, L2 and L3 with respect to σ_2 for $\bar{\Omega}$=2.8283

highly divergent and hence unstable with respect to L4 and L5. The Jacobi constant C is determined as follows,

$$\bar{v}^2 - \frac{\bar{\Omega}^2}{2}(\bar{x}^2 + \bar{y}^2) - \frac{\sigma_1}{\bar{r}_1} - \frac{\sigma_2}{\bar{r}_2} = C \tag{2.31}$$

where, $\bar{v}$= speed of the spacecraft relative to the rotating frame of reference. In order to determine regions of zero-velocity and restricted motion (i.e. $z = 0$), the equation for the Jacobi Constant becomes,

$$C = -\frac{\bar{\Omega}^2}{2}(\bar{x}^2 + \bar{y}^2) - \frac{\sigma_1}{\bar{r}_1} - \frac{\sigma_2}{\bar{r}_2} \tag{2.32}$$

Three of the Jacobi constants are determined by plugging in the co-ordinates of the Lagrangian points L1, L2 and L3 respectively. The Jacobi regions are then plotted using the values of these constants. The Jacobi regions of the Earth-Moon-Spacecraft system are presented in Figures 2.7-2.9 In the given plots, the region between the inner and outer boundaries represents the forbidden region i.e., inaccessible for an Earth launched spacecraft. As the value of C increases the forbidden region shrinks. The two inner lobes in Figure 2.7 depict the Earth and Moon. Further, the Jacobi regions for the restricted three body case discussed are explored.

Figure 2.10 present the plots of the Jacobi regions for a symmetric case i.e., $\sigma_1 = \sigma_2 = 0.5$ at $\bar{\Omega} = 1$. It is to be noted that the lobes in this case are equal and symmetrical corresponding to the equal mass ratios.

The asymmetric case is then analyzed (Figures 2.11), i.e., for a sample case of $\sigma_1 = 2/3$, $\sigma_2 = 1/3$ at $\bar{\Omega} = 1$. Here again, it is to be noted that the lobes in this case are unequal and asymmetrical corresponding to the unequal mass ratios.
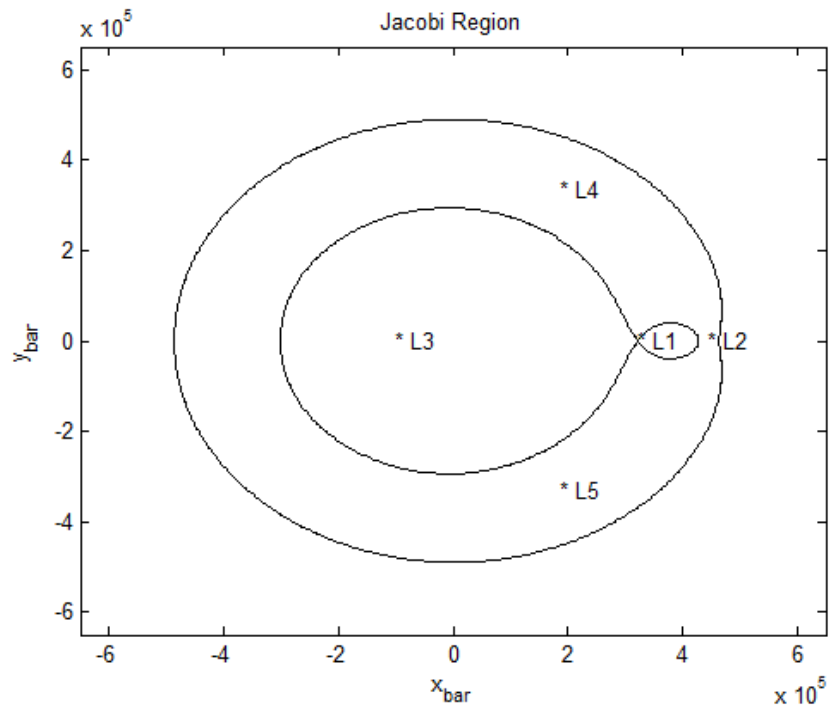
Figure 2.7. Jacobi regions for $C_1 = $ -1.6735
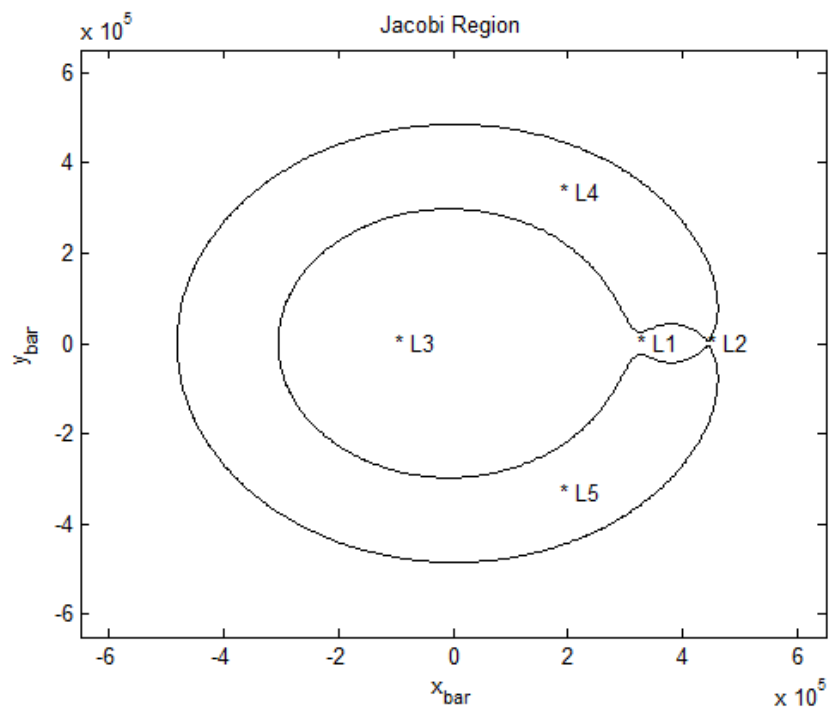
Figure 2.8. Jacobi regions for $C_2 = $ -1.6649
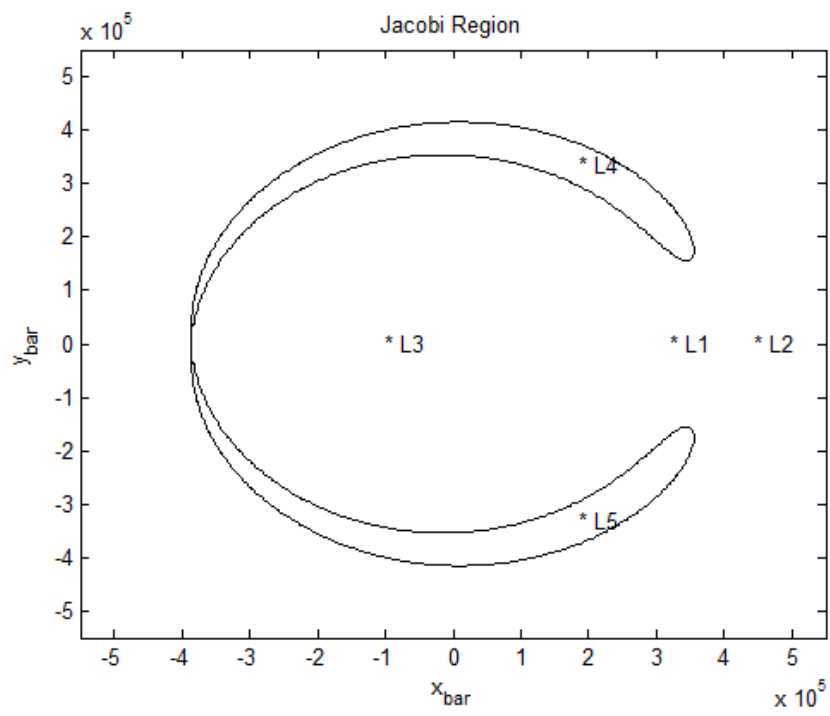
Figure 2.9. Jacobi regions for $C_3 = $ -1.5810
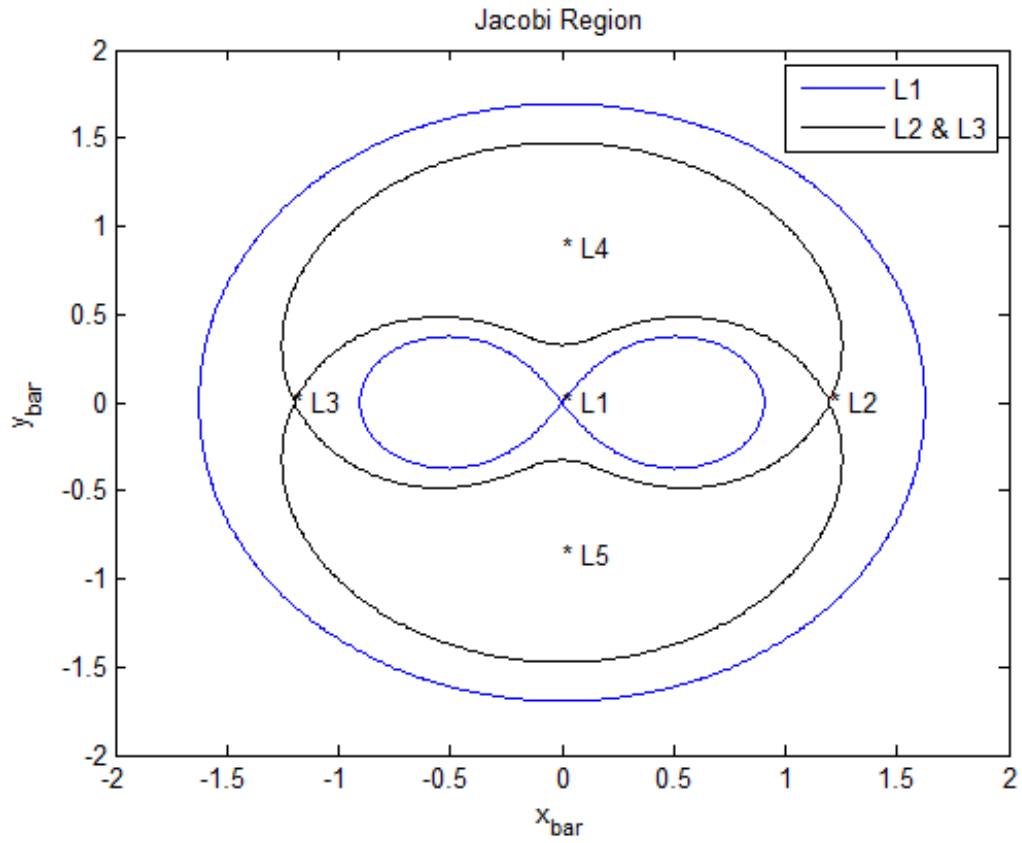
Figure 2.10. Jacobi regions for $C_1 = $ -2 at L1 ($\bar{x} = 0$) and $C_{2,3} = -1.728398$ at L2,3 ($\bar{x} = \pm 1.1984$)
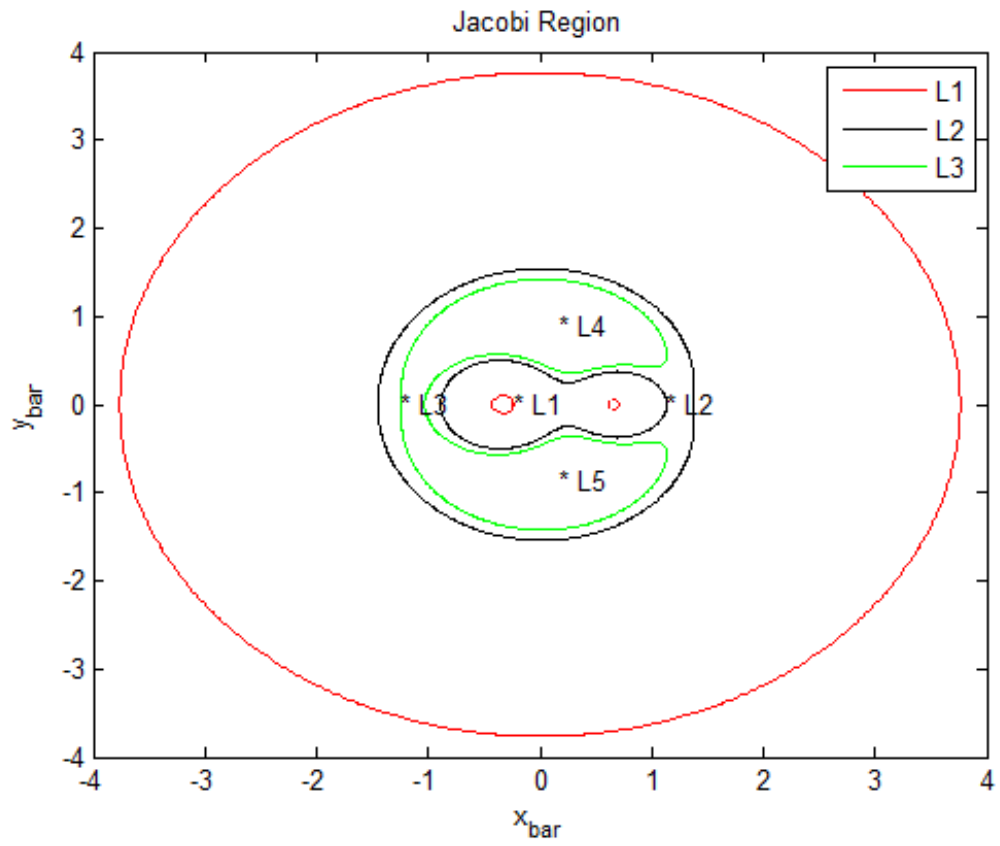
Figure 2.11. Jacobi regions for $C_1 = $ -7.346154 at L1 ($\bar{x} = $ -0.2374), $C_2 = $ -1.808990 at L2 ($\bar{x} = $ 1.1363) and $C_3 = $ -1.682071 at L3 ($\bar{x} = $ -1.2490)

3. THE ASTEROID RESTRICTED FOUR BODY PROBLEM

3.1   Introduction

Let us extend the restricted three body problem to a four body case. The reason behind this, is to provide further understanding of the multi-body modeling, as additional masses are added to the existing system. Let us consider a system of three spheres (primary masses) and a spacecraft (secondary mass). All assumptions remain exactly as those of the three body case. In addition r_{13} is the distance between the centers of spheres 1 and 3. Below are presented three different configurations of the four body case.
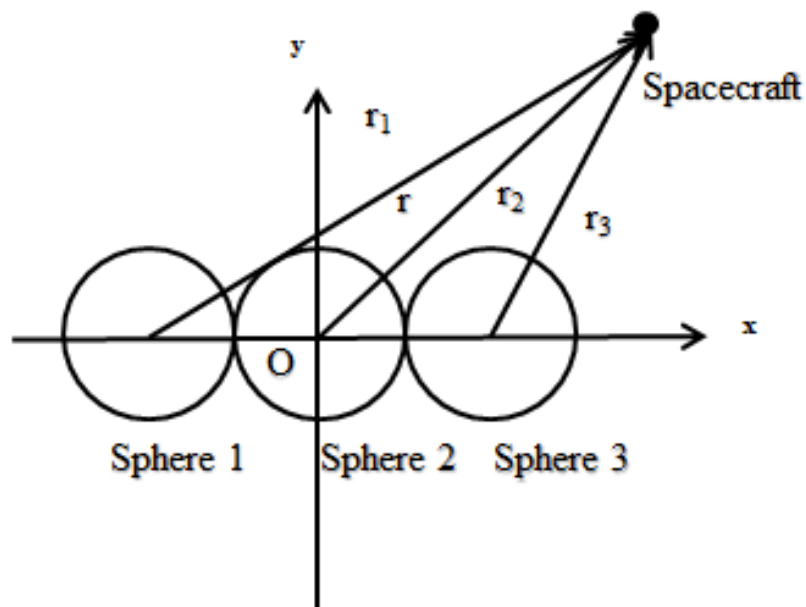
Figure 3.1. Symmetric configuration of a sphere system with equal mass ratios
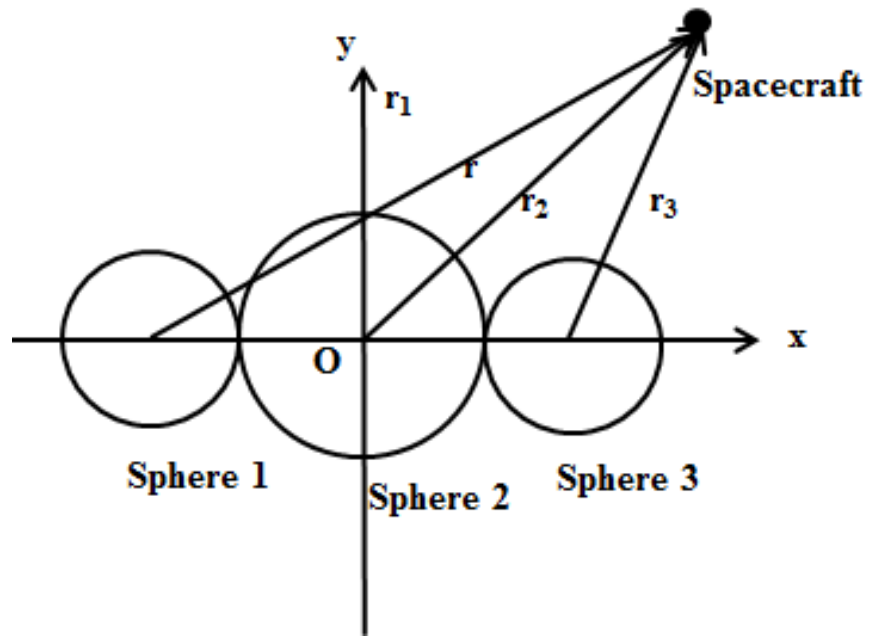
Figure 3.2. Symmetric configuration of a sphere system with unequal mass ratios
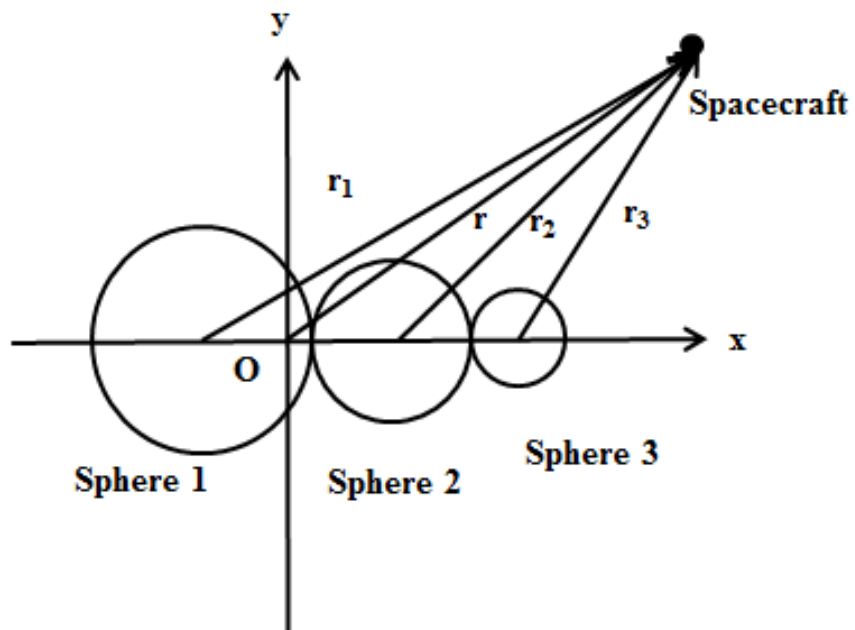
Figure 3.3. Asymmetric configuration of a sphere system with decreasing mass ratios

3.2   Equations of Motion

As the previous case, the gravitational potential is used to derive the equations of motion. The non-dimensionalized equations of motion are presented below. It is to be noted that the overbar notation is omitted for the sake of convenience. All distances for this case are non-dimensionalized with respect to r_{13} and σ_3 is the mass ratio of the third mass.

$$\ddot{x} - 2\Omega\dot{y} - \Omega^2 x = -\frac{\sigma_1}{r_1^3}(x + \sigma_{23}) - \frac{\sigma_2}{r_2^3}(x - R + \sigma_{23}) - \frac{\sigma_3}{r_3^3}(x - 1 + \sigma_{23}) \tag{3.1}$$

$$\ddot{y} + 2\Omega\dot{x} - \Omega^2 y = -\frac{\sigma_1}{r_1^3}y - \frac{\sigma_2}{r_2^3}y - \frac{\sigma_3}{r_3^3}y \tag{3.2}$$

$$\ddot{z} = -\frac{\sigma_1}{r_1^3}z - \frac{\sigma_2}{r_2^3}z - \frac{\sigma_3}{r_3^3}z \tag{3.3}$$

where,

$$R = r_{12}/r_{13}$$

$$\sigma_{23} = \sigma_2 R + \sigma_3$$

$$r_{12} = \frac{(\frac{\sigma_1}{\sigma_3})^{\frac{1}{3}} + (\frac{\sigma_2}{\sigma_3})^{\frac{1}{3}}}{(\frac{\sigma_1}{\sigma_3})^{\frac{1}{3}} + 2(\frac{\sigma_2}{\sigma_3})^{\frac{1}{3}} + 1}$$

An important inference here, is that addition of another mass led to just addition of a single term and did not change the nature of the existing equation in terms of degree and order. This is the prime advantage of the multi-body modeling approach. It does not increase the complexity of the equations as further terms are added due to addition of more masses. This reduces the computation time.

3.3 Lagrangian Points

The Lagrangian points are determined next from the above equations of motion, in the same manner as carried out previously. All the Lagrangian points in this case have no analytic solutions. The equations solved simultaneously to obtain L4 and L5 are as follows.

$$\Omega^2 x = -\frac{\sigma_1}{r_1^3}(x + \sigma_{23}) - \frac{\sigma_2}{r_2^3}(x - R + \sigma_{23}) - \frac{\sigma_3}{r_3^3}(x - 1 + \sigma_{23}) \tag{3.4}$$

$$\Omega^2 y = -\frac{\sigma_1}{r_1^3}y - \frac{\sigma_2}{r_2^3}y - \frac{\sigma_3}{r_3^3}y \tag{3.5}$$

The following table presents the values of co-ordinates of L4 and L5 for Ω=1, for different configurations. The points are obtained using numerical methods.

The first case shown in the table represents the case of the three spheres such that they have decreasing masses and thus an asymmetric configuration. The second case represents the symmetric configuration of the three spheres such that the mass of the central sphere is twice that of the two adjacent spheres. The x-co-ordinate is observed to be at zero, corresponding to the symmetry of the configuration. The third case is a test of the approach as the one of the masses is set to zero i.e., a return to the three body problem. The results confirm with those of the three body symmetric case for $\Omega = 1$ i.e., $\simeq (0, \frac{\sqrt{3}}{2})$. The last case is just an observation of the change in results when the zero mass is replaced by a very small mass.

The remaining equilibrium points, L1, L2 and L3 are then determined from the Equation 3.6 following the previous procedure.

Table 3.1. Co-ordinates of L4 and L5 for $\Omega = 1$, for different configurations of mass ratios

Distance between C.O.M	Mass Ratios	L4,L5
$r_{13} = 1$ $r_{12} = 0.5384$	$\sigma_1 = 0.50$ $\sigma_2 = 0.30$ $\sigma_3 = 0.20$	0.0817, 0.9233
$r_{13} = 1$ $r_{12} = 0.5$	$\sigma_1 = 0.25$ $\sigma_2 = 0.50$ $\sigma_3 = 0.25$	0, 0.9456
$r_{13} = 1$ $r_{12} = 0.5$	$\sigma_1 = 0.50$ $\sigma_2 = 0$ $\sigma_3 = 0.50$	0.0001,0.8660
$r_{13} = 1$ $r_{12} = 0.5013$	$\sigma_1 = 0.50$ $\sigma_2 = 0.01$ $\sigma_3 = 0.49$	0.0049,0.8681

$$\ddot{x} - 2\Omega\dot{y} - \Omega^2 x = -\frac{\sigma_1}{r_1^3}(x + \sigma_{23}) - \frac{\sigma_2}{r_2^3}(x - R + \sigma_{23}) - \frac{\sigma_3}{r_3^3}(x - 1 + \sigma_{23}) \qquad (3.6)$$

where,

$$r_1 = |x + \sigma_{23}|; r_2 = |x - R + \sigma_{23}|; r_3 = |x - 1 + \sigma_{23}|$$
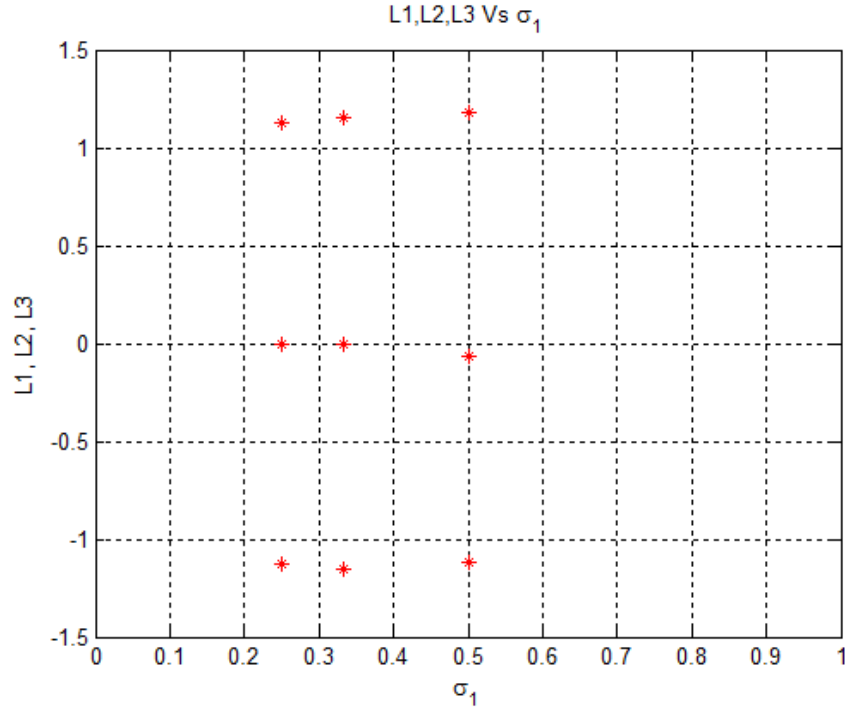
Figure 3.4. Plot of x-co-ordinates of L1, L2 and L3 with respect to σ_1 for $\Omega = 1$ for $\sigma_1 = 0$, 1/3, 2/3; $\sigma_2 = 1/3$; $\sigma_3 = 1 - \sigma_2 - \sigma_3$

From the plot in Figure 3.4 we observe the values of L1, L2 and L3 for $\Omega = 1$ for the three discussed configurations. For the symmetric cases it is observed that L1 lies at $x = 0$.

3.4 Jacobi Analysis

The Jacobi constants and their corresponding Jacobi regions are determined for the Lagrangian points L1, L2 and L3. The equation solved for obtaining the Jacobi Constant is as follows.

$$C = -\frac{\Omega^2}{2}(x^2 + y^2) - \frac{\sigma_1}{r_1} - \frac{\sigma_2}{r_2} - \frac{\sigma_3}{r_3} \tag{3.7}$$

The plots below represent the Jacobi regions for all the three configurations discussed. The asymmetric case is analyzed, i.e. for a sample case of $\sigma_1 = 0.5$, $\sigma_2 = 0.3$ and $\sigma_3 = 0.2$ at $\Omega = 1$. It is to be noted that the lobes in this case (Figure 3.5) are unequal and asymmetrical corresponding to the unequal mass ratios and three different Jacobi regions are generated corresponding to the three unique Jacobi integrals

The symmetric configuration of the three spheres of equal masses i.e. $\sigma_1 = \sigma_2 = \sigma_3 = 1/3$ at $\Omega = 1$ is next. It is to be noted that the lobes in this case (Figure 3.6) are equal and symmetrical corresponding to the equal mass ratios. Also it is observed the Jacobi regions are identical corresponding to the symmetric Lagrangian roots L2 and L3.

Finally the other symmetric configuration, corresponding to $\sigma_1 = \sigma_3 = 0.25$, $\sigma_2 = 0.5$; at $\Omega = 1$, is analyzed. Here again, it is observed that the central lobe in Figure 3.7 is larger than the adjacent lobes in accordance with the above mentioned mass ratios. Also the Jacobi regions are identical due to their symmetric roots.
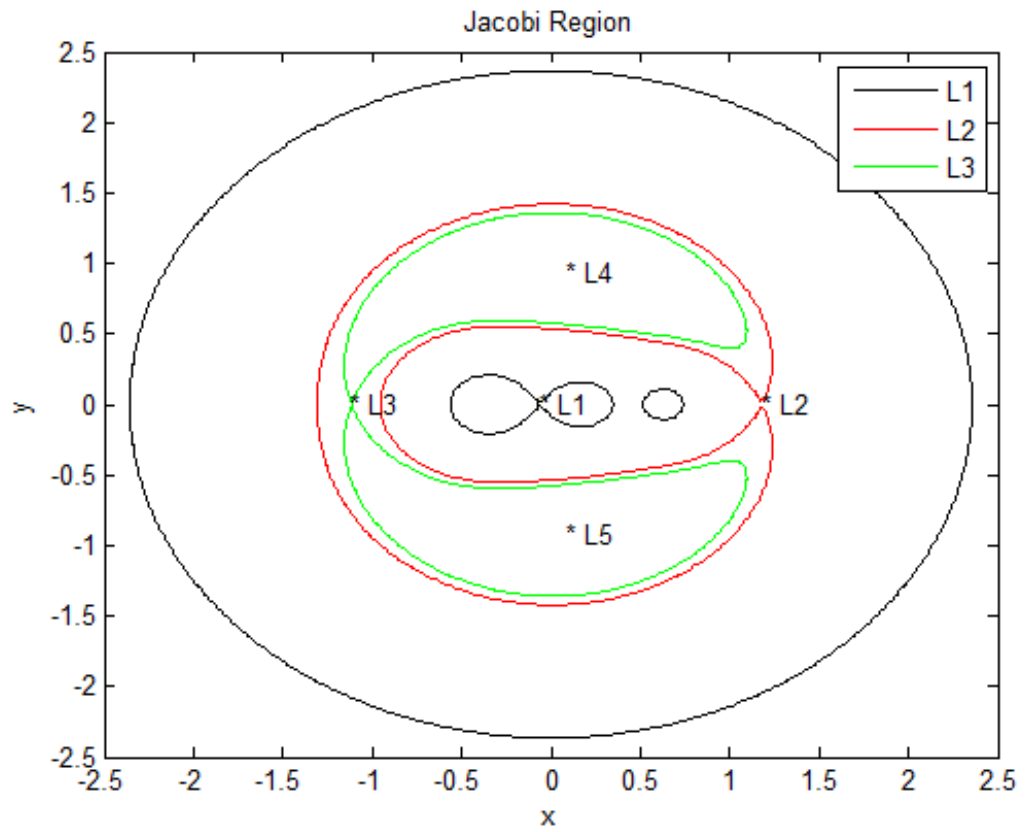
Figure 3.5. Jacobi regions for C_1 = -3.212439 at L1 (x = -0.0624), C_2 = -1.688938 at L2 (x = 1.1824) and C_3 = -1.631470 at L3 (x = -1.1179)
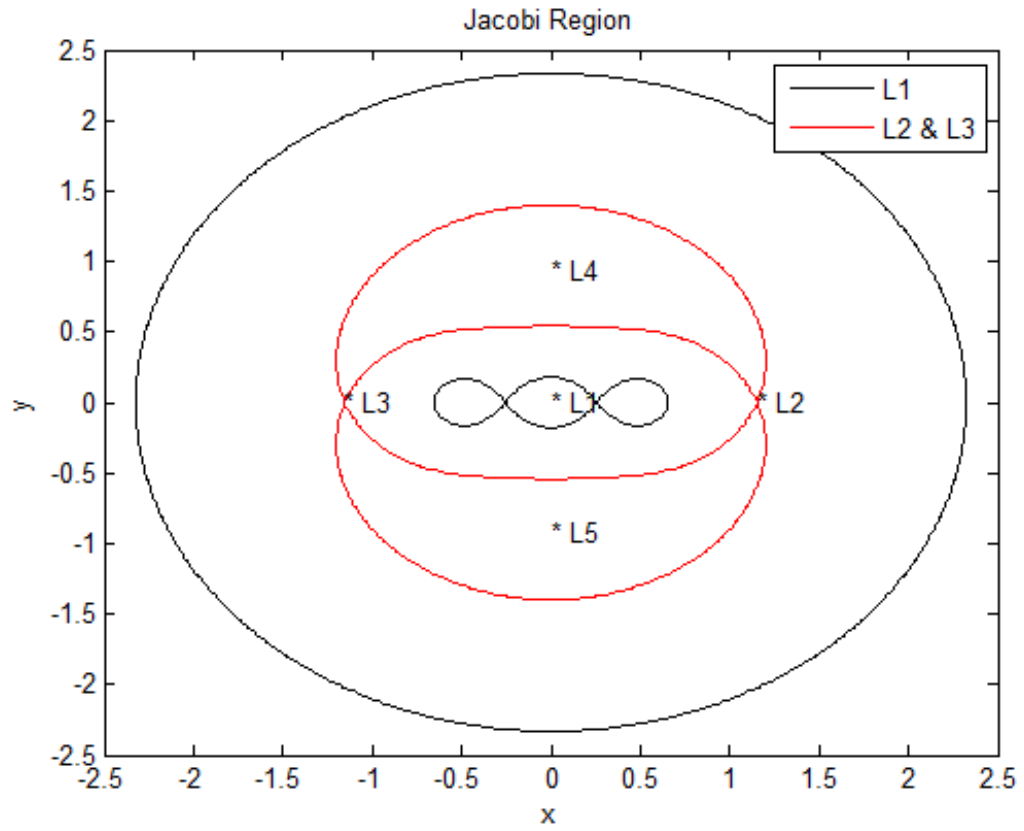
Figure 3.6. Jacobi regions for C_1 = -3.141694 at L1 ($x = 0$) and $C_{2,3}$ = -1.665923 at L2,3 ($x = \pm 1.1534$)
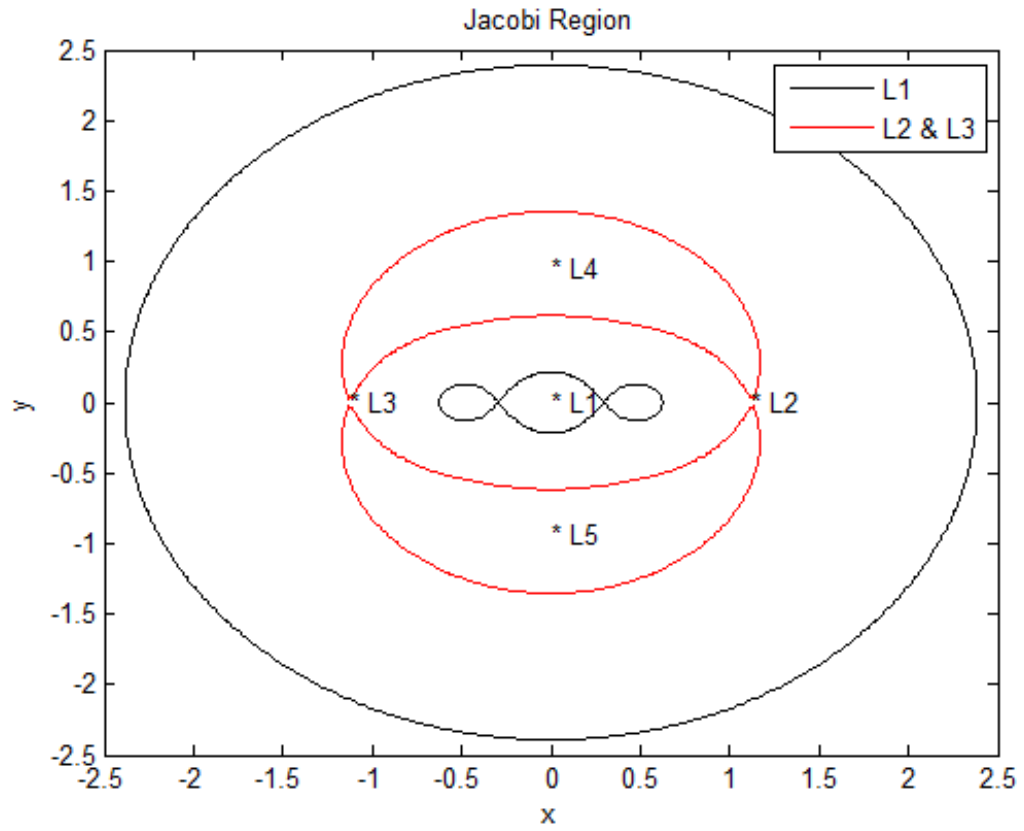
Figure 3.7. Jacobi regions for $C_1 = $ -3.272352 at L1 ($x = 0$) and $C_{2,3}$ = -1.6311 at L2,3 ($x = \pm 1.1262$)

4. THE SPHERICAL HARMONICS APPROACH

4.1 Introduction

So far the multi-body modeling approach was discussed. One of the most commonly used approaches to model gravity fields of irregularly shaped bodies is the spherical harmonics modeling approach. This approach is just a solution to the Laplace equation corresponding to physical mass distribution. It is used to model irregular shaped bodies, in our case asteroids. It utilizes harmonic co-efficients to model the irregularities, choosing them to match with the actual potential function. Spherical harmonics is applied to model the gravity fields of planets too. For example, the Earth although generally treated as a sphere for the purpose of computation of gravity potential, is more of a spheroid in actual as are other planets, hence spherical harmonics could model the gravity potential more accurately. This however, is a series expansion and hence results in minor truncation errors.

An important drawback of this approximation is that, it does not take mass distribution into account. Spherical harmonics approximates an irregular body based on a constant density assumption. In general, asteroids have non uniform mass distribution. Hence spherical harmonics holds good from a far field point of view, but diverges in the vicinity of the asteroid.

The gravitational potential is given by the following approximation,(Scheeres, 2012)

$$U(r, \delta, \lambda) = \frac{\mu}{r} \sum_{l=0}^{\infty} \sum_{l=0}^{l} (\frac{r_o}{r})^l P_{lm}(sin\delta)[C_{lm}cosm\lambda + S_{lm}sinm\lambda] \qquad (4.1)$$

where,

r_o = normalizing radius of the body

P_{lm} = Associated Legendre Functions

C_{lm}, S_{lm} = Gravity field harmonic co-efficients

$r^2 = x^2 + y^2 + z^2; sin\delta = \frac{z}{r}; tan\lambda = \frac{y}{x}$

Let us apply this approach to a symmetrical body, example an ellipsoid, to understand the modeling approach better. An ellipsoid is a closed quadric surface that is a three-dimensional analogue of an ellipse. The standard equation of an ellipsoid centered at the origin of a Cartesian coordinate system and aligned with the axes is,

$$\frac{x^2}{a^2} + \frac{y^2}{b^2} + \frac{z^2}{c^2} = 1 \qquad (4.2)$$

where, a, b and c are the semi major, intermediate and minor axes respectively.

Let us consider a constant density ellipsoid, rotating with an angular speed $\Omega\hat{k}$. A spacecraft orbits this ellipsoid in a *restricted plane i.e., x-y plane*. Further, the ellipsoid is an ellipsoid of revolution i.e., *b=c*. The motive to model the ellipsoid with these restrictions is to later investigate the convergence of Lagrangian points yielded with the solutions of the symmetric configuration of the Restricted Four body Problem where $\sigma_1 = \sigma_3$, at $\Omega = 1$, since the ellipsoid can be approximated by this configuration as shown in the next chapter. Further, the ellipsoid has a closed form solution and

hence owing to its symmetry would be easier to analyze using the spherical harmonics approach.
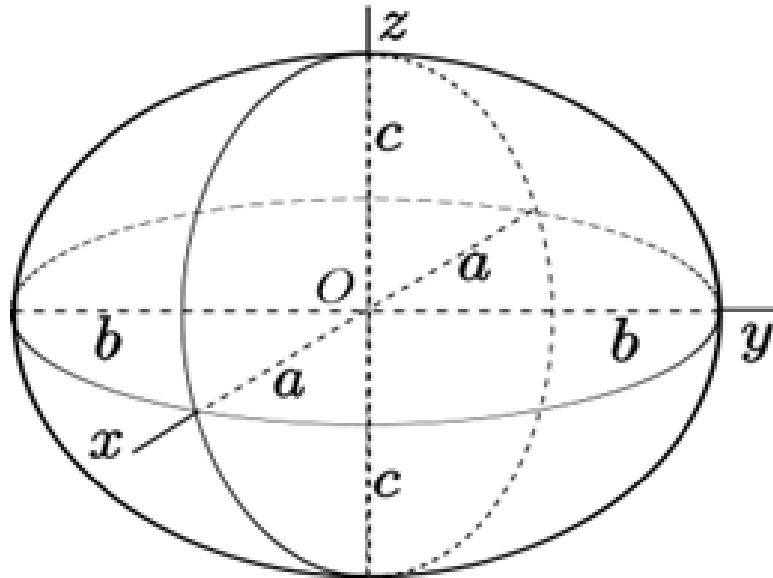
Figure 4.1. Tri-axial Ellipsoid with semi axes a, b and c marked (Mercator, 2010)

4.2 Gravitational Potential

The gravitational potential is computed from Equation 4.1. It is to be noted that the series can be expanded to infinite number of terms. However this is unrealistic and hence the series is truncated to a particular order and degree. The accuracy of the approximation is proportional to the number of terms included in the series expansion. Generally, the co-efficients up to the quadratic term are more significant and hence it is common practice to expand the series up to the second order. However, in order to increase the accuracy let us expand the series to the fourth order. It is

important to remember that, the greater the irregularity of the body, greater is the order of expansion required for the above series.

The expression to determine the Gravity harmonic co-efficients for a constant density (σ) body is given as follows (Montenbruck & Gilll, 2000).

$$(C,S)_{lm} = \frac{\sigma(2-\delta_m^0)}{M}\frac{(l-m)!}{(n+m)!}\int_S \frac{R^3(\delta,\lambda)}{l+3}(\frac{R(\delta,\lambda)}{r_o})^l P_{lm}(sin\delta)cos(m\delta)cos\delta d\delta d\lambda$$

(4.3)

where, the radius $R(\delta,\lambda)$ is a function of the latitude and longitude and defines the shape of the body.

Several of the above Gravity field harmonic co-efficients reduce to zero under the following conditions. $C_{00} = 1$ by definition. If the origin is chosen to be at the center of mass, $C_{11} = S_{11} = C_{10} = 0$ due to the following definition.

$$x_{CM} = C_{11}r_o$$

$$y_{CM} = S_{11}r_o$$

$$z_{CM} = C_{10}r_o$$

Secondly, for any given mass distribution, it is always possible to define a set of coordinates such that the products of the polar moments of inertia i.e. I_{xy}, I_{yz} and I_{zx} are zero. The polar moments of inertia are defined as follows.

$$I_{xy} = -2Mr_o^2 S_{22}$$

$$I_{yz} = -Mr_o^2 S_{21}$$

$$I_{zx} = -Mr_o^2 C_{21}$$

From the above definitions, $S_{22} = S_{21} = C_{21} = 0$. Thirdly, due to the symmetry of the ellipsoid, all the S_{lm} co-efficients reduce to zero. Further if either l or m is odd, $C_{lm} = 0$. Thus we are left with the following truncated approximation up to the fourth order.

$$U = \frac{\mu}{r}\{P_{00}(sin\delta)C_{00} + (\frac{r_o}{r})^2[P_{20}(sin\delta)C_{20} + P_{22}(sin\delta)C_{22}cos2\lambda]+$$
$$(\frac{r_o}{r})^4[P_{40}(sin\delta)C_{40} + P_{42}(sin\delta)C_{42}cos2\lambda + P_{44}(sin\delta)C_{44}cos4\lambda]\}$$

(4.4)

The Associated Legendre Polynomials are derived from the following expression,

$$P_{lm}(sin\delta) = cos^m\delta \sum_{i=0}^{int[l-\frac{m}{2}]} T_{lmi}sin^{l-m-2i}\delta$$

(4.5)

where,

$$T_{lmi} = \frac{(-1)^i(2l-2i)!}{2^l i!(l-2i)!(l-m-2i)!}$$

where, the $int[x]$ functions returns the integer part of x. The associated Legendre functions can also be defined by the following simpler rule, for a general case.

$$P_{lm}(x) = (1-x^2)^{m/2}\frac{d^m}{dx^m}(P_{l0}(x))$$

(4.6)

where,

$$P_{l0} = \frac{1}{2^l l!}\frac{d^l}{dx^l}(x^2-1)^l$$

The restricted motion (x-y plane) imposes the following conditions.

$$z = 0 \tag{4.7}$$

This implies the following,

$$sin\delta = 0 \tag{4.8}$$

$$cos\lambda = \frac{x}{r} \tag{4.9}$$

$$r^2 = x^2 + y^2 \tag{4.10}$$

$$P_{lm}(sin\delta) = P_{lm}(0) \tag{4.11}$$

Further, the simplified expressions of the Gravity field harmonic co-efficients for a constant density ellipsoid are as follows.

$$C_{20} = \frac{1}{5r_o^2}(c^2 - \frac{a^2 + b^2}{2}) \tag{4.12}$$

$$C_{22} = \frac{1}{20r_o^2}(a^2 - b^2) \tag{4.13}$$

$$C_{40} = \frac{15}{7}(C_{20}^2 + 2C_{22}^2) \tag{4.14}$$

$$C_{42} = \frac{5}{7}C_{20}C_{22} \tag{4.15}$$

$$C_{44} = \frac{5}{28}C_{22}^2 \tag{4.16}$$

Substituting the above assumptions and, the values of the harmonic co-efficients and associated Legendre polynomials, we get the following expression for the gravitational potential.

$$U = \frac{\mu}{r}\{1 + (\frac{r_o}{r})^2[\frac{-C_{20}}{2} + 3C_{22}\frac{x^2 - y^2}{r^2}]$$
$$+(\frac{r_o}{r})^4[\frac{C_{40}}{8} - \frac{15}{2}C_{42}\frac{x^2 - y^2}{r^2} + 105C_{44}\frac{x^4 - 6x^2y^2 + y^4}{r^4}]\} \tag{4.17}$$

4.3   Equations of Motion

As discussed in the three and four body problems, the non-dimensionalized equations of motion are derived from the gradient of the gravitational potential and presented below. The normalizing variables are r_o, Ω_c and t_c .

$$\ddot{x} - 2\Omega\dot{y} - \Omega^2 x = -\frac{\mu x}{r^3}\{1 - 3(\frac{r_o}{r})^2[\frac{-C_{20}}{2} + 3C_{22}\frac{7y^2 - 3x^2}{r^2}]+$$
$$(15\frac{r_o}{r})^4[\frac{C_{40}}{8} - \frac{C_{42}}{2}\frac{9y^2 - 5x^2}{r^2} + 7C_{44}\frac{5x^4 - 46x^2y^2 + 21y^4}{r^4}]\} \tag{4.18}$$

$$\ddot{y} + 2\Omega\dot{x} - \Omega^2 y = -\frac{\mu y}{r^3}\{1 - 3(\frac{r_o}{r})^2[\frac{-C_{20}}{2} + 3C_{22}\frac{3y^2 - 7x^2}{r^2}]+$$
$$(15\frac{r_o}{r})^4[\frac{C_{40}}{8} - \frac{C_{42}}{2}\frac{5y^2 - 9x^2}{r^2} + 7C_{44}\frac{5y^4 - 46x^2y^2 + 21x^4}{r^4}]\} \tag{4.19}$$

$$z = 0 \tag{4.20}$$

From the above equations, it is evident that the nature of the terms becomes increasingly complex as the order of expansion increases. Further, the above equations are much more complex than those obtained as a result of multi-sphere modeling.

4.4   Lagrangian Points

Although Lagrangian points traditionally exist in three body problems, their existence is investigated, for an ellipsoid using spherical harmonics. According to

D.J.Scheeres, four equilibrium points are yielded by spherical harmonics approxima-
tion for the general case of asteroids with the exception of the asteroid *Betulia* which
yields six such points. The procedure adopted for determining these points is as per
the previous cases. The time-invariant equations solved to get the equilibrium points
are given below.

$$\Omega^2 = -\frac{\mu}{r^3}\{1 - 3(\frac{r_o}{r})^2[\frac{-C_{20}}{2} + 3C_{22}\frac{7y^2 - 3x^2}{r^2}]+$$
$$(15\frac{r_o}{r})^4[\frac{C_{40}}{8} - \frac{C_{42}}{2}\frac{9y^2 - 5x^2}{r^2} + 7C_{44}\frac{5x^4 - 46x^2y^2 + 21y^4}{r^4}]\}$$
(4.21)

$$\Omega^2 = -\frac{\mu}{r^3}\{1 - 3(\frac{r_o}{r})^2[\frac{-C_{20}}{2} + 3C_{22}\frac{3y^2 - 7x^2}{r^2}]+$$
$$(15\frac{r_o}{r})^4[\frac{C_{40}}{8} - \frac{C_{42}}{2}\frac{5y^2 - 9x^2}{r^2} + 7C_{44}\frac{5y^4 - 46x^2y^2 + 21x^4}{r^4}]\}$$
(4.22)

$$z = 0$$
(4.23)

The above equations were solved using numerical methods for a sample case of $a = 3, b = 2, c = 1 = r_o$ to obtain symmetrical roots for L4 and L5, $[0, \pm1.3886]$ shown in
Figure 4.4.

Further, the existence of the collinear equilibrium points is investigated by setting
$y = 0$, reducing the above system of equations to the following.

$$\Omega^2 = -\frac{\mu}{r^3}\{1 - 3(\frac{r_o}{r})^2[\frac{-C_{20}}{2} + 3C_{22}\frac{7y^2 - 3x^2}{r^2}]+$$
$$(15\frac{r_o}{r})^4[\frac{C_{40}}{8} - \frac{C_{42}}{2}\frac{9y^2 - 5x^2}{r^2} + 7C_{44}\frac{5x^4 - 46x^2y^2 + 21y^4}{r^4}]\}$$
(4.24)

where, $r = |x|$. Two equilibrium points, $(\pm1.67839, 0)$ are obtained by solving the
above equation for the same conditions.
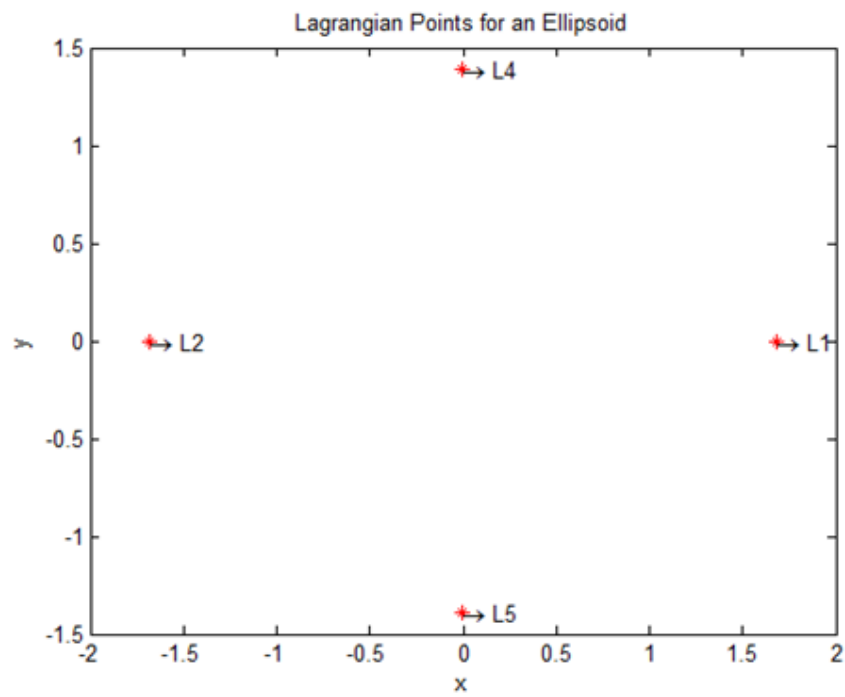
Figure 4.2. Lagrangian Points for an ellipsoid, $a = 3, b = 2, c = 1 = r_o$

5. VALIDATION

The asteroid gravitational potential modeling techniques - Multiple body modeling ans Spherical harmonics were studied in detail in the previous chapters. The prime focus of this thesis is to present the technique of multi-sphere modeling as it is computationally less demanding and also takes into account mass distribution when compared to spherical harmonics. To effectively substitute the spherical harmonics approximation with multiple sphere modeling, the convergence of the Lagrangian points yielded by both methods, was investigated.

For this purpose, an ellipsoid was modeled as a cluster of three spheres and Lagrangian points were computed through both the discussed approaches and the percentage difference was calculated. The motive for this, is to be able to model any asymmetric body, an asteroid in our case, by a cluster of spheres in contact with each other and rotating with a constant angular speed about their common center of mass.

The spheres can be cotangent or overlapping. Further each sphere can have a unique size and density. For modeling the cluster as an ellipsoid a symmetric configuration of three spheres - a central large sphere and the symmetric smaller adjacent spheres, as discussed in the Four body problem. The case of overlapping spheres is not considered for the sake of simplicity.

In order to approximate an ellipsoid as a cluster of cotangent spheres, mass and moment of inertia have to be conserved. Based on this, the dimensions and mass distribution of the spheres is computed. Since the bulk of the matter of an ellipsoid is concentrated at the center, the density of the central sphere is the same as that of the ellipsoid ρ_e and the radius of the sphere is the the length of the semi major axis of the ellipsoid b. It is for this reason that an ellipsoid of revolution $(b = c)$ was considered, since a sphere is fitted in its center. Further, spheres 1 and 3 have equal dimensions R_{S1}, density ρ_1 and mass M_{S1} due to symmetry.
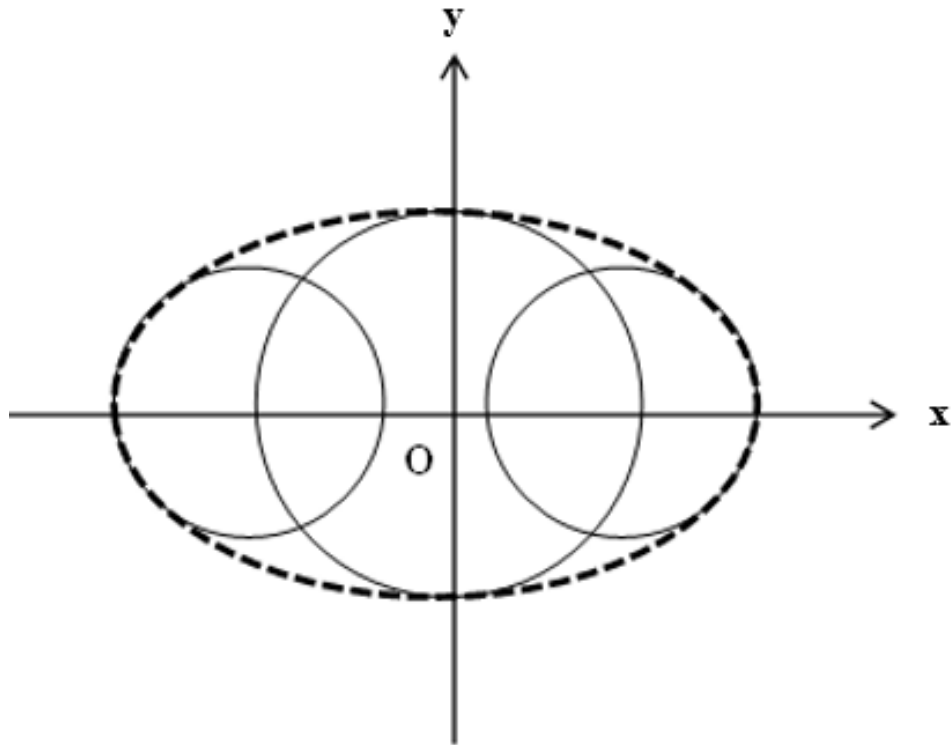
Figure 5.1. Approximation of an ellipsoid using three spheres with non-uniform individual sphere density

The following equations present the mass and moment of inertia conservation.
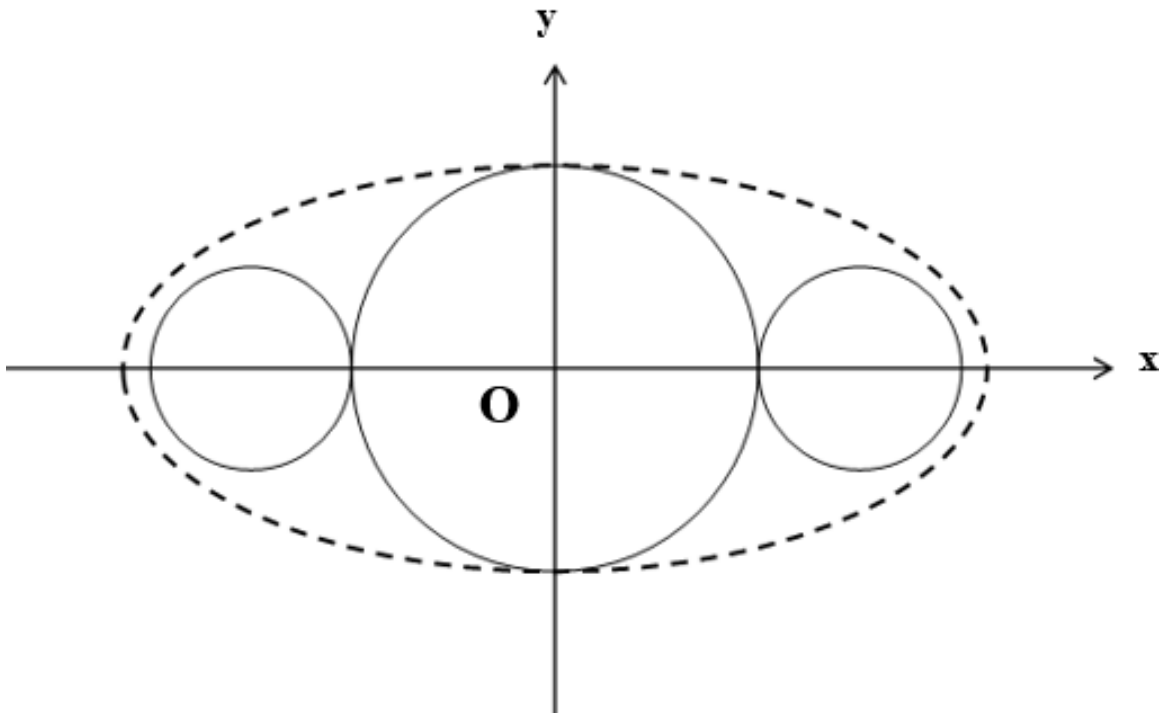
Figure 5.2. Approximation of an ellipsoid using three cotangent spheres for uniform individual sphere density

Mass Conservation:

$$M_e = M_{S2} + 2M_{S1} \tag{5.1}$$

where,

M_e = Mass of the Ellipsoid

M_{S1}, M_{S2} = Mass of spheres 1 and 2 respectively

$$\rho_e V_e = \rho_e V_{S2} + 2\rho_1 V_{S1} \tag{5.2}$$

where,

V_{S1}, V_{S2} = Volume of spheres 1 and 2 respectively

$$\frac{7}{5}(1-b)R_{S1}^2 + 2b(1-b)R_{S1} + b^2(1-b) - \frac{1}{5}(1-b^2) = 0 \tag{5.3}$$

Moment of Inertia Conservation:

$$I_{zz,e} = I_{zz,S2} + 2(I_{zz,S1} + M_{S1}r_{12}^2) \tag{5.4}$$

$$\frac{1}{5}\rho_e V_e(a^2 + b^2) = \frac{1}{5}\rho_e V_{S2}R_{S1}^2 + 2(\frac{1}{5}\rho_1 V_{S1}(R_{S1} + b)^2) \tag{5.5}$$

where,

$I_{zz,e}$ = Moment of Inertia of the Ellipsoid

$I_{zz,S1}, I_{zz,S2}$ = Moment of Inertia of spheres 1 and 2 respectively

Based on equations 5.3 and 5.5, R_{S1} and ρ_1 are plotted as a function of b. It is to be noted that all the equations (5.1-5.5) are non-dimensional. Densities are

normalized with respect to ρ_e and distances are normalized with respect to the semi-major axis length of the ellipsoid a. Figures 5.3 and 5.4 represent the variation of R_{S1} and ρ_1 with b
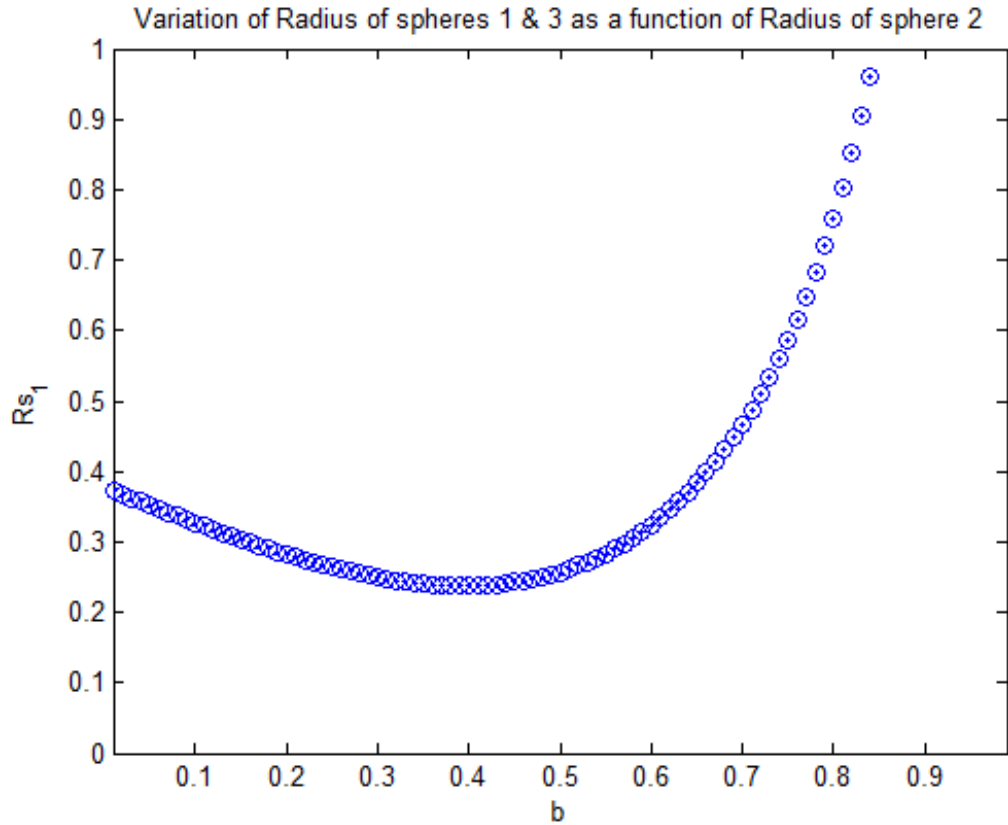
Figure 5.3. Variation of R_{S1} with b

As a test case, a sample value was picked for b, and the corresponding values of R_{S1} and ρ_1 were obtained from the plots in Figures 5.3 and 5.4. For $b = 0.4a$, $R_{S1} = 0.23775a$ and $\rho_1 = 3.5718\rho_e$. Lagrangian points were determined as done in the case of the Asteroid Restricted Problem using equations 3.4-3.6. Also the Lagrangian
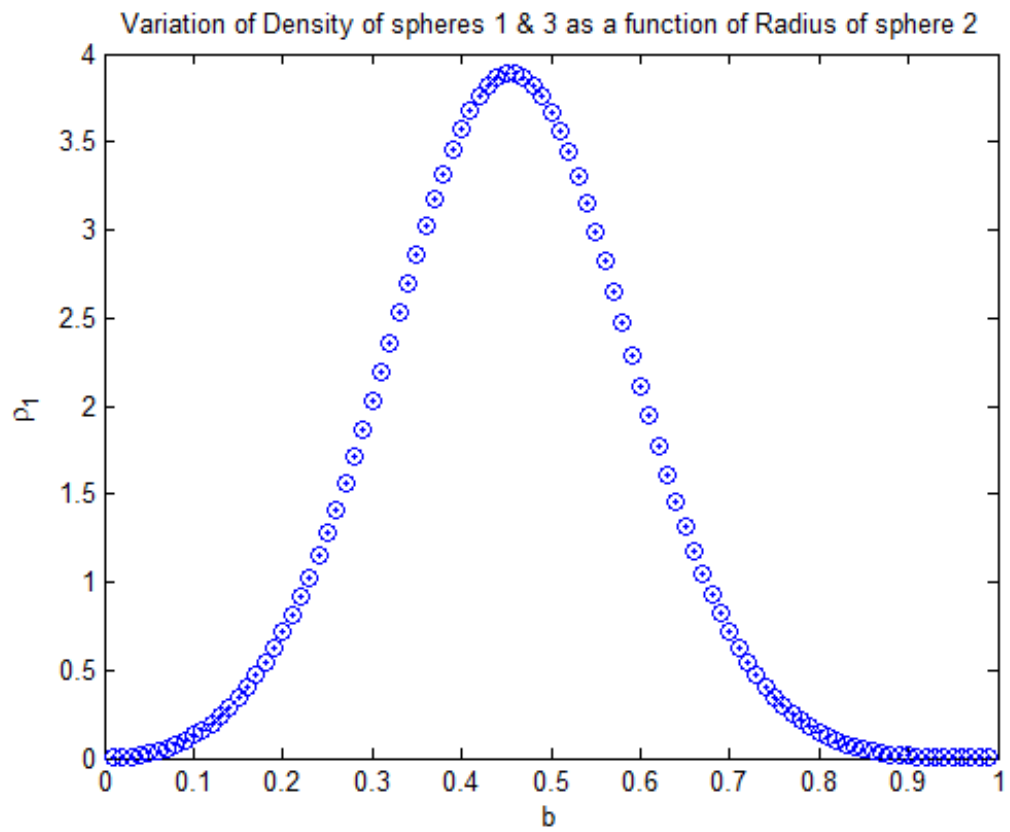
Figure 5.4. Variation of ρ_1 with b

Table 5.1. Lagrangian Points for an Ellipsoid modeled as a cluster of spheres

Lagrangian Point	Multiple-body modeling	Spherical Harmonics	% difference
L1	0.2706, 0	N/A	N/A
L2	+1.1430, 0	+1.1563, 0	1.16%
L3	-1.1430, 0	-1.1563, 0	1.16%
L4	0, +0.9324	0, +0.9506	1.93%
L5	0, -0.9324	0, -0.9506	1.93%

points through spherical harmonics approximation were determined using equations 4.21-4.24. Table 5.1 presents the values of the obtained equilibroum points for the discussed test case.

From Table 5.1, it is observed that the percentage difference between the Lagrangian points obtained from both techniques ranges from 1.16-1.93%, indicating that multiple sphere modeling can very closely approximate the spherical harmonics approximation.

6. CONCLUSIONS

This thesis focused on modeling asteroid gravitational potentials. The first part of the thesis focused on the approach of multiple-body or more specifically multiple sphere modeling. To get a good understanding of this approach, Asteroid Restricted Three and Four body problems where studied. Using the above modeling approach, the gravitational potential for both problems was computed, for symmetric and asymmetric configurations. This provides further insight into modeling a single asteroid as a cluster of spheres in contact with each other. Further, it was inferred from the nature of the equations of motion that, as additional masses were considered in the cluster, each mass added a corresponding additional term with similar structure, to the existing equations of motion. This is the biggest advantage of multiple body modeling. The computation of the gravitational potential facilitated the determination of equilibrium positions i.e. Lagrangian points and also the Jacobi regions (forbidden regions) corresponding to the unstable Lagrangian Points.

The second approach that was investigated is the spherical harmonics modeling. This is an existing approach. It was applied to obtain gravitational potential for an ellipsoid. Spherical harmonics, being an approximation, loses its accuracy upon truncation. Besides, as the order of expansion is increased, the nature of the additional terms increases in complexity. This is an important demerit of this approach. Loss

of accuracy and increased complexity reduce the favorability of spherical harmonics modeling.

Another important parameter that was studied was mass distribution. Spherical Harmonics approximations, like elliptic integrals and polyhedron models, approximates an asymmetric body as a constant density mass. This assumption holds good from a far field point of view, however, inside the Brillouin sphere (circumscribing sphere for the asteroid), the approximations diverge. Further, many asteroids have non-homogeneous mass distributions. Mascon model takes mass distribution into account as does multiple body modeling. Multi-sphere modeling however accounts for moment of inertia conservation which is not taken into consideration in the mascon model.

A demerit of multi-sphere modeling and mascon model is that, they require a lot of topological and density variation data of the asteroid considered, to approximate it with multiple masses. Since, only a few asteroids like Ceres, Eros, etc have been fully studied and only triaxial dimensions and overall density are known for other asteroids, it is an important drawback of this concept.

As a final step, to validate the accuracy of multiple sphere, the convergence of Lagrangian points yielded by this method and by spherical harmonics, was investigated. The percentage difference between the two methods was between 1.16-1.93% indicating that for the purpose of determination of Lagrangian points, multi-sphere modeling can closely approximate spherical harmonics.

REFERENCES

C. Magri, D. S. e. a., S.J. Ostro. (2007). *Radar observations and a physical model of asteroid 1580 betulia.* Icarus, 186: 152-177.

Curtis, H. D. (2010). *Orbital mechanics for engineering students* (Second ed.). Burlington, MA: Elsevier.

Danby, J. (1962). *Fundamentals of celestial mechanics.* New York, USA: Macmillan.

E. Herrera Sucarrat, P. P., & Roberts, R. (2013). *Modeling the gravitaional potential of a nonspherical asteroid.* University of Surrey, England, UK: Journal of Guidance, Control and Dynamics, Vol. 36, No. 3.

Hu, W., & Scheeres, D. J. (2002). *Spacecraft motion about slowly rotating asteroids.* Journal of Guidance, Control and Dynamics, Vol. 25, No. 4.

Hu, W., & Scheeres, D. J. (2004). *Numerical determination of stability regions for orbital motion in uniformly rotating second degree and order gravity fields.* Planetary and Space Science, Vol. 52, No. 8.

Lowry, S. C. (2014). Asteroid itokawa [Computer software manual]. University of Kent, UK. Retrieved from `http://newspoint.co.za/story/414/5356-asteroid-itokawa-s-different-parts-varies-densities`

Mercator, P. (2010). Ellipsoid [Computer software manual]. Retrieved from `https://en.wikipedia.org/wiki/Ellipsoid`

Montenbruck, O., & Gilll, E. (2000). *Satellite orbits: Models, methods, applications.* New York, USA: Springer.

Nermiroff, R., & Bonnell, J. (2014). Asteroid itokawa [Computer software manual]. ASD at NASA/GSFC. Retrieved from `http://apod.nasa.gov/apod/ap140209.html`

P. Geissler, J. P. e. a. (1996). *Erosion and erecta reaccretion on 243 ida and its moon.* Icarus, Vol. 120, No. 1.

Scheeres, D. J. (1994). *Dynamics about uniformly rotating triaxial ellipsoids: Application to asteroids.* Icarus, Vol. 110, No. 2.

Scheeres, D. J. (2009). *Stability of the planar full 2 - body problem.* Celestial Mechanics and Dynamical Astronomy Vol. 104, Nos. 1-2.

Scheeres, D. J. (2012). *Orbital motion in strongly perturbed environments : Applications to asteroid, comet and planetary satellite orbiters.* New York, USA: Springer.

S.J. Ostro, D. J. S. e. a. (1996). *Orbits close to the asteroid 4769 castalia.* Icarus, Vol. 121, No. 1.

Szebehely, V. (1967). *Modeling the gravitaional potential of a nonspherical asteroidtheory of orbits: The restricted problem of three bodies.* New York, USA: Academic Press Inc.

Werner, R. A. (1993). *The gravitational potential of a homogeneous polyhedron or don't cut corners.* Austin, Texas: Celestial Mechanics and Dynamical Astronomy 59:253-278.

Werner, R. A. (1997). *Spherical harmonic coefficientsfor the potential of a constant - density polyhedron.* Computers and Geosciences, 23(10):1071-1077.

Werner, R. A., & Scheeres, D. J. (1996). *Exterior gravitation of a polyhedron derived and compared with harmonic and mascon gravitation representations of asteroid 4769 castalia.* Jet Propulsion laboratory, California: Celestial Mechanics and Dynamical Astronomy 65:313-344.

Werner, R. A., & Scheeres, D. J. (2005). *Mutual potential of homogeneous polyhedra.* Celestial Mechanics and Dynamical Astronomy 91:337-349.

A. MATLAB CODES

A.1 The Asteroid Restricted Three Body Problem

A.1.1 Determination of Lagrangian Points - L4 and L5

```matlab
% Program to determine the Lagrangian points L4 and L5 for an
% Asteroid Restricted Three Body Problem
clc
clear all

omega = 0:0.05:3; %...omega is non domensional
y =  sqrt( ((1./omega).^(4./3)) - 0.25 ); %...y is non-dimensional

plot(omega,y,'k')
hold on
plot(omega,-y,'k')

xlabel('\Omega_b_a_r');
ylabel('y_b_a_r');
title('y vs \Omega for L4, L5');
```

A.1.2 Determination of Lagrangian Points - L1, L2 and L3

```matlab
% Program to determine the Lagrangian points L1, L2 and L3 for an
% Asteroid Restricted Three Body Problem

clc
clear all
close all
global sigma1 sigma2 Omega

% r12_dim = distance between the centers of the two masses
% r12 = non-dimensional r12_dim
% r12 = 1;

% Mass Ratios
% sigma1 = m1/(m1 + m2)
% sigma2 = m2/(m1 + m2)
```

```matlab
16  % sigma1 + sigma2 = 1
17
18  for sigma1 = 0:0.1:1;
19  sigma2 = 1 - sigma1;
20
21  % Omega_dim = dimensional angular speed of the two primary masses, which
22  % can be either detached or rigidly attached
23  % Omega = non-dimensional angular speed of the two primary masses
24
25  % nc = dimensional angular speed of the two primaries when they are not
26  % rigidly attached
27  % Omega = Omega_dim/nc
28
29  % We start with Omega = 1
30  Omega = 1; % Omega = 2, 2.8283
31
32  % All x distances are non-dimensional
33  % x is non-dimensional coordinate defined as:
34  % x_dim = r12_dim*x
35
36  x10 = 0;
37  xL(1) = fminsearch('LHS_of_Eq1',x10)
38  F1 = LHS_of_Eq1(xL(1))
39
40  x20 = 3;
41  xL(2) = fminsearch('LHS_of_Eq1',x20)
42  F2 = LHS_of_Eq1(xL(2))
43
44  x30 = -3;
45  xL(3) = fminsearch('LHS_of_Eq1',x30)
46  F3 = LHS_of_Eq1(xL(3))
47
48  hold on
49  plot(sigma2, xL, 'k-*')
50  xlabel('\sigma_2');
```

A.1.3   Determination of Lagrangian Points - L1, L2 and L3 - Function file

```matlab
1  function [F] = LHS_of_Eq1(x)
2  % All x distances are non-dimensional
3  % x is non-dimensional coordinate defined as:
4  % x_dim = r12_dim*x
5
6  global sigma1 sigma2 Omega
7  r1 = abs(x + sigma2); %..Position Vector of Sphere1
8  r2 = abs(x - sigma1); %..Position Vector of Sphere2
9
10  r1_3 = r1.^3;
11  r2_3 = r2.^3;
```

```
12
13 f1 = sigma1.*(x + sigma2)/r1_3 + sigma2.*(x - sigma1)/r2_3 - x.*Omega^2;
14 F = f1.^2;
15 end
```

A.1.4 Determination of Jacobi Integral

```
1  % Determination of Jacobi Constants C1, C2 & C3
2  % from x-y co-ordinates of L1, L2 & L3 respectively
3  clc
4  clear all
5
6  % Solving for an Earth-Moon system for verification
7  % All Equations used are non-dimensionalized
8  % i.e length with respect to r12 & omega with respect to 'nc'
9
10 % Equation to solve for C is as follows
11 % C = 0.5*(omega^2)*(x^2 + y^2) - sigma1/r1 - sigma2/r2
12
13 %Basic Data for an Earth-Moon system from Dr.Curts's book
14
15 % nc = 2.66538e-6;%rad/s...Asteroid rotation rate
16 % omega_dim = 2.66538e-6;%rad/s...Asteroid rotation rate
17 % omega = omega_dim/nc...Hence omega = 1
18
19 % r12 = 3.844e+5;%km...Distance between centers of mass
20 % of the two bodies
21 % x_dim(L1) = 0.8369*r12
22 % x(L1) = x_dim(L1)/r12 = 0.8369
23 % y_dim(L1) = 0*r12
24 % y(L1) = y_dim(L1)/r12 = 0
25
26 omega = 1;
27
28 x = 0.8369;
29 y = 0;
30
31 sigma1 = 0.9878;% mass ratio m1/(m1 + m2)
32 sigma2 = 1 - sigma1;% mass ratio m1/(m1 + m2)
33
34 %Position vectors
35 r1 = sqrt( (x + sigma2).^2 + y.^2 );%km
36 r2 = sqrt( (x - sigma1).^2 + y.^2 );%km
37
38 C = -(0.5*(omega^2)*(x^2 + y^2)) - (sigma1/r1) - (sigma2/r2);
39
40 fprintf('The Jacobi Constant is %2.6f',C);
```

A.1.5 Determination of Jacobi Regions

```matlab
1  % Program to plot Jacobi Regions
2
3  clc
4  clear all
5  clf
6
7  ezplot('JacobiRegion',[-5.5e5 5.5e5]);
8  setcurve('color','black')
9  hold on
10
11 % ezplot('JacobiRegion23',[-2 2]);
12 % setcurve('color','black')
13
14
15 % ezplot('JacobiRegion33',[-2 2]);
16 % setcurve('color','green')
17
18 title('Jacobi Region')
19 xlabel('x_{bar}');
20 ylabel('y_{bar}');
21 legend('L1','L2','L3')
22
23 % Labelling the Lagrangian Points
24 x1 = 0;
25 y1 = 0;
26 str1 = '* L1';
27 text(x1,y1,str1)
28
29 x2 = 1.1984;
30 y2 = 0;
31 str2 = '* L2';
32 text(x2,y2,str2)
33
34 x3 = -1.1984;
35 y3 = 0;
36 str3 = '* L3';
37 text(x3,y3,str3)
38
39 x4 = 0;
40 y4 = 0.8661;
41 str4 = '* L4';
42 text(x4,y4,str4)
43
44 x5 = 0;
45 y5 = -0.8661;
46 str5 = '* L5';
47 text(x5,y5,str5)
```

A.1.6 Determination of Jacobi Regions - Function file

```matlab
1  function F = JacobiRegion(x,y)
2
3  %Basic Data for an Earth—Moon System
4  % C = −1.6649; % Jacobi Constant
5  % omega = 2.66538e−6;%rad/s  Asteroid rotation rate
6  % r12 = 3.844e+5;%km     Distance between centers of mass of the two bodies
7  % myu1 = 398620;%km^3/s^2   Gravitaional constant of the first body
8  % myu2 = 4903.02;%km^3/s^2  Gravitaional constant of the second body
9  % sigma2 = 0.01215;        % mass ratio m1/(m1 + m2)
10 % sigma1 = 1 − sigma2;     % mass ratio m1/(m1 + m2)
11
12 % For the sphere system
13 omega = 1;%rad/s          Asteroid rotation rate
14 sigma1 = 2/3;             % mass ratio m1/(m1 + m2)
15 sigma2 = 1 − sigma1;     % mass ratio m1/(m1 + m2)
16
17 %Position vectors
18 r1 = sqrt( (x+sigma2).^2 + y.^2 );%km
19 r2 = sqrt( (x−sigma1).^2 + y.^2 );%km
20
21 %Defining terms of the equation
22 Eq1_t1 = (omega^2)*(x.^2 + y.^2);
23 Eq1_t2 = 2*sigma1./r1;
24 Eq1_t3 = 2*sigma2./r2;
25 Eq1_t4 = 2*C;
26
27 F = Eq1_t1 + Eq1_t2 + Eq1_t3 + Eq1_t4;
28
29 end
```

A.2 The Asteroid Restricted Four Body Problem

A.2.1 Determination of Lagrangian Points - L4 and L5

```matlab
1  % Program to determine the Lagrangian points L4 and L5 for an
2  % Asteroid Restricted Four Body Problem
3  clc
4  clear all
5  close all
6  global r13 r12 sigma1 sigma2 sigma3 Omega
7
8  % Mass Ratios
9  % sigma1 = m1/(m1 + m2 + m3)
```

```
10  % sigma2 = m2/(m1 + m2 + m3)
11  % sigma3 = m2/(m1 + m2 + m3)
12  % sigma1 + sigma2 + sigma3 = 1
13
14  sigma1 = 1/3;
15  sigma2 = 1/3;
16  sigma3 = 1 - sigma1 - sigma2;
17
18  % r13_dim = distance between the centers of masses 1 and 3
19  % r13 = non-dimensional r13_dim
20  % r12_dim = distance between the centers of masses 1 and 2
21  % r12 = non-dimensional r12_dim
22  % r13 = Rs1 + 2*Rs2 + Rs3...Rs is radius of a sphere
23  % r12 = Rs1 + Rs2
24  % sigma1/sigma3 = m1/m3 = (Rs1/Rs3)^3...Constant Density Assumption
25  % sigma1/sigma2 = m1/m2 = (Rs1/Rs2)^3...Similarly
26
27  r13 = 1;
28  r12 = ((sigma1/sigma3)^(1/3) + (sigma2/sigma3)^(1/3))/...
29  ((sigma1/sigma3)^(1/3) + 2*(sigma2/sigma3)^(1/3) + 1);
30
31  % Omega_dim = dimensional angular speed of the two primary masses, which
32  % can be either detached or rigidly attached
33  % Omega = non-dimensional angular speed of the two primary masses
34
35  % nc = dimensional angular speed of the two primaries when they are not
36  % rigidly attached
37  % Omega = Omega_dim/nc
38
39  Omega = 1;
40
41  X0 = [-10;10];
42  XL = fminsearch('Four_body_LHS_of_Eq1_2',X0)
43  G = Four_body_LHS_of_Eq1_2(XL)
```

A.2.2 Determination of Lagrangian Points - L4 and L5 - Function file

```
1  function [F] = Four_body_LHS_of_Eq1_2(X)
2
3  % All x distances are non-dimensional
4  % x is non-dimensional coordinate defined as:
5  % x_dim = r13_dim*x
6
7  global r13 r12 sigma1 sigma2 sigma3 Omega
8
9  %Short hand notation
10  R = r12/r13;
11  sigma23 = sigma2*R + sigma3;
12
```

```
13  x = X(1);
14  y = X(2);
15
16  r1 = sqrt( (x + sigma23)^2 + y^2 );
17  r2 = sqrt( (x - R + sigma23)^2 + y^2 );
18  r3 = sqrt( (x - 1 + sigma23)^2 + y^2 );
19
20  r1_3 = r1^3;
21  r2_3 = r2^3;
22  r3_3 = r3^3;
23
24  f1 = sigma1*(x + sigma23)/r1_3 + ...
25  sigma2*(x - R + sigma23)/r2_3  + ...
26  sigma3*(x - 1 + sigma23)/r3_3 - x*Omega^2;
27  f2 = sigma1/(r1_3) + sigma2/(r2_3) + sigma3/(r3_3) -Omega^2;
28
29  LHS_Eq1_Sqrd = f1^2;
30  LHS_Eq2_Sqrd = f2^2;
31
32  F = max(LHS_Eq1_Sqrd, LHS_Eq2_Sqrd);
33  end
```

A.2.3   Determination of Lagrangian Points - L1, L2 and L3

```
1  % Program to determine the Lagrangian points L1, L2 and L3 for an
2  % Asteroid Restricted Four Body Problem
3  clc
4  clf
5  global r13 r12 sigma1 sigma2 sigma3 Omega
6
7  sigma1 = 1/3;
8  sigma2 = 1/3;
9  sigma3 = 1 - sigma1 - sigma2;
10
11 r13 = 1;
12 r12 = ( ((sigma1/sigma3)^(1/3)) + ((sigma2/sigma3)^(1/3)) )/...
13 (((sigma1/sigma3)^(1/3)) + (2*(sigma2/sigma3)^(1/3)) + 1 );
14
15 Omega = 1;
16
17 x10 = -1e-20;
18 xL(1) = fminsearch('Four_body_LHS_of_Eq1',x10)
19 F1 = Four_body_LHS_of_Eq1(xL(1))
20
21 x20 = 1;
22 xL(2) = fminsearch('Four_body_LHS_of_Eq1',x20)
23 F2 = Four_body_LHS_of_Eq1(xL(2))
24
25 x30 = 3;
```

```
26  xL(3) = fminsearch('Four_body_LHS_of_Eq1',x30)
27  F3 = Four_body_LHS_of_Eq1(xL(3))
28
29  x40 = -1;
30  xL(4) = fminsearch('Four_body_LHS_of_Eq1',x40)
31  F4 = Four_body_LHS_of_Eq1(xL(4))
32
33  x50 = -3;
34  xL(5) = fminsearch('Four_body_LHS_of_Eq1',x50)
35  F5 = Four_body_LHS_of_Eq1(xL(5))
36
37  plot(sigma1,xL,'k*')
38  hold on
39
40  title('L1,L2,L3 Vs \sigma_1');
41  xlabel('\sigma_1');
42  ylabel('L1, L2, L3');
43  axis([0 1 -1.5 1.5])
```

A.2.4 Determination of Lagrangian Points - L1, L2 and L3 - Function file

```
1  function [F] = Four_body_LHS_of_Eq1(x)
2
3  global r13 r12 sigma1 sigma2 sigma3 Omega
4
5  %Short hand notation
6  R = r12/r13;
7  sigma23 = sigma2*R + sigma3;
8
9  r1 = abs(x + sigma23);
10  r2 = abs(x - R + sigma23);
11  r3 = abs(x - 1 + sigma23);
12
13  r1_3 = r1.^3;
14  r2_3 = r2.^3;
15  r3_3 = r3.^3;
16
17  f1 = sigma1*(x + sigma23)/r1_3 +...
18  sigma2*(x - R + sigma23)/r2_3  +...
19  sigma3*(x - 1 + sigma23)/r3_3 - x.*Omega^2;
20
21  F = f1^2;
22  end
```

A.2.5 Determination of Jacobi Integral

```matlab
1  % Determination of Jacobi Constants C1, C2 & C3
2  % from x—y co—ordinates ol L1, L2 & L3 respectively
3  clc
4  clear all
5
6  % Equation to solve for C is as follows
7  % C = 0.5*(omega^2)*(x^2 + y^2) — sigma1/r1 — sigma3/r3
8
9  omega = 1;
10
11 x = 0.0001;
12 y = 0;
13
14 sigma1 = 0.5;% mass ratio m1/(m1 + m2 + m3)
15 sigma2 = 0;% mass ratio m2/(m1 + m2 + m3)
16 sigma3 = 1 — sigma1 — sigma2;% mass ratio m3/(m1 + m2 + m3)
17
18 r13 = (sigma1/sigma3)^(1/3) + 2*(sigma2/sigma3)^(1/3) + 1;
19 r12 = (sigma1/sigma3)^(1/3) + (sigma2/sigma3)^(1/3);
20
21 %Short hand notation
22 R = r12/r13;
23 sigma23 = sigma2*R + sigma3;
24
25 %Position vectors
26 r1 = sqrt( (x + sigma23)^2 + y^2 );
27 r2 = sqrt( (x — R + sigma23)^2 + y^2 );
28 r3 = sqrt( (x — 1 + sigma23)^2 + y^2 );
29
30 C = —(0.5*(omega^2)*(x^2 + y^2)) — (sigma1/r1) ...
31 — (sigma2/r2) — (sigma3/r3);
32
33 fprintf('The Jacobi Constant is %2.6f',C);
```

A.2.6 Determination of Jacobi Regions

```matlab
1  % Determination of Jacobi Regions for an
2  % Asteroid Restricted Four Body Problem
3  clc
4
5  ezplot('JacobiRegion_Four_Body_Case',[—2.5 2.5]);
6  setcurve('color','black')
7  hold on
8
9  xlabel('x');
10 ylabel('y');
11
12 % ezplot('JacobiRegion_Four_Body_Case23',[—2.5 2.5]);
13 % setcurve('color','red')
```

```matlab
14
15  % ezplot('JacobiRegion_Four_Body_Case33',[-2.5 2.5]);
16  % setcurve('color','green')
17
18  legend('L1','L2 & L3')
19  title('Jacobi Region')
20
21  % Labelling the Lagrangian Points
22  x1 = 0;
23  y1 = 0;
24  str1 = '* L1 ';
25  text(x1,y1,str1)
26
27  x2 = 1.1534;
28  y2 = 0;
29  str2 = '* L2 ';
30  text(x2,y2,str2)
31
32  x3 = -1.1534;
33  y3 = 0;
34  str3 = '* L3 ';
35  text(x3,y3,str3)
36
37  x4 = 0;
38  y4 = 0.9231;
39  str4 = '* L4 ';
40  text(x4,y4,str4)
41
42  x5 = 0;
43  y5 = -0.9231;
44  str5 = '* L5 ';
45  text(x5,y5,str5)
```

A.2.7   Determination of Jacobi Regions - Function file

```matlab
1   function F = JacobiRegion_Four_Body_Case(x,y)
2
3   C = -1.6311;                  % Jacobi Constant
4   omega = 1;%rad/s              Asteroid rotation rate
5
6   sigma1 = 0.25;  % mass ratio m1/(m1 + m2 + m3)
7   sigma2 = 0.5;   % mass ratio m2/(m1 + m2 + m3)
8   sigma3 = 1 - sigma1 - sigma2;  % mass ratio m3/(m1 + m2 + m3)
9
10  r13 = (sigma1/sigma3)^(1/3) + 2*(sigma2/sigma3)^(1/3) + 1;
11  r12 = (sigma1/sigma3)^(1/3) + (sigma2/sigma3)^(1/3);
12
13  %Short hand notation
14  R = r12/r13;
```

```matlab
15  sigma23 = sigma2*R + sigma3;
16
17  %Position vectors
18  r1 = sqrt( (x + sigma23).^2 + y.^2 );
19  r2 = sqrt( (x - R + sigma23).^2 + y.^2 );
20  r3 = sqrt( (x - 1 + sigma23).^2 + y.^2 );
21
22  %Defining terms of the equation
23  Eq1_t1 = (omega^2)*(x.^2 + y.^2);
24  Eq1_t2 = 2*sigma1./r1;
25  Eq1_t3 = 2*sigma2./r2;
26  Eq1_t4 = 2*sigma3./r3;
27  Eq1_t5 = 2*C;
28
29  F = Eq1_t1 + Eq1_t2 + Eq1_t3 + Eq1_t4 + Eq1_t5;
30
31  end
```

A.3   Spherical Harmonics Modeling

A.3.1   Determination of Lagrangian Points of an Ellipsoid

```matlab
1   % Program  to determine the Lagrangian points of an Ellipsoid
2   clc
3   clear all
4   close all
5
6   global Omega
7
8   % r0_dim = Characteristic radius of the Ellipsoid
9   % r0 = non-dimensional r0_dim
10  % Omega_dim = dimensional angular speed of the ellipsoid
11  % Omega = non-dimensional angular speed of the ellipsoid
12
13  % All x and r distances are non-dimensional
14  % x is non-dimensional coordinate defined as:
15  % x_dim = r0_dim*x
16  % r_dim = r0_dim*x
17  % Omega is non dimensional
18  % Omega_dim = OmegaC_dim*Omega
19
20  Omega = 1;
21
22  % To determine L4 and L5 for the Ellipsoid
23
24  X10 =[0;-1.38]
25  XL = fminsearch('Lagrangian_Points_Ellipsoid',X10)
26  G1 = Lagrangian_Points_Ellipsoid(XL)
27
```

```matlab
28  plot(XL(1),XL(2),'r*')
29  hold on
30
31  X20 =[0;1.38]
32  XL = fminsearch('Lagrangian_Points_Ellipsoid',X20)
33  G2 = Lagrangian_Points_Ellipsoid(XL)
34
35  plot(XL(1),XL(2),'r*')
36  hold on
37  title('Lagrangian Points for an Ellipsoid');
38  ylabel('y');
39  xlabel('x');
40
41  % To determine L1 and L2 for the Ellipsoid
42
43  x11 = 0;
44  xL1(1) = fminsearch('Lagrangian_Points_L123_Ellipsoid',x11)
45  F1 = Lagrangian_Points_L123_Ellipsoid(xL1(1))
46
47  x21 = 3;
48  xL1(2) = fminsearch('Lagrangian_Points_L123_Ellipsoid',x21)
49  F2 = Lagrangian_Points_L123_Ellipsoid(xL1(2))
50
51  x31 = 5;
52  xL1(3) = fminsearch('Lagrangian_Points_L123_Ellipsoid',x31)
53  F3 = Lagrangian_Points_L123_Ellipsoid(xL1(3))
54
55  x41 = -3;
56  xL1(4) = fminsearch('Lagrangian_Points_L123_Ellipsoid',x41)
57  F4 = Lagrangian_Points_L123_Ellipsoid(xL1(4))
58
59  x51 = -5;
60  xL1(5) = fminsearch('Lagrangian_Points_L123_Ellipsoid',x51)
61  F5 = Lagrangian_Points_L123_Ellipsoid(xL1(5))
62
63  y = 0;
64  plot(xL1,y,'r*')
65
66  % Point Labels
67
68  x1 = 1.6783;
69  y1 = 0;
70  str1 = '\rightarrow L1';
71  text(x1,y1,str1)
72
73  x2 = -1.6783;
74  y2 = 0;
75  str2 = '\rightarrow L2';
76  text(x2,y2,str2)
77
78  x4 = -0.0001;
79  y4 = 1.3886;
```

```
80  str4 = '\rightarrow L4';
81  text(x4,y4,str4)
82
83  x5 = −0.0001;
84  y5 = −1.3886;
85  str5 = '\rightarrow L5';
86  text(x5,y5,str5)
```

A.3.2   Determination of Lagrangian Points - L4 and L5 - Function file

```
1   % Function file for determining Lagrangian Points for an Ellipsoid
2
3   % The equations of motion are as follows
4   % Omega^2−[(1/r^3)*{1 − (3/r^2)*[ C20/2 + C22*(7*y^2 − 3*x^2)/r^2 ]..
5   % + (15/r^4)*[ C40/8 + 0.5*C42(9*y^2 − 5*x^2)/r^2 + ...
6   % 7*C44*(5*x^4 −46x^2*y^2 + 21*y^4)/r^2 ]} = 0...eq(1)
7
8   % Omega^2−[(1/r^3)*{1 − (3/r^2)*[ C20/2 + C22*(3*y^2 − 7*x^2)/r^2 ]..
9   % + (15/r^4)*[ C40/8 + 0.5*C42(5*y^2 − 9*x^2)/r^2 + ...
10  % 7*C44*(5*y^4 −46x^2*y^2 + 21*x^4)/r^2 ]} = 0...eq(2)
11  function F = Lagrangian_Points_Ellipsoid(X)
12
13  global Omega
14
15  % Special case 1:
16  % a, b and c are non−dimensional a_bar = a/r0
17  b = 2;
18  c = 1;
19  a = 3;
20
21  C20 = 0.2*(c^2 − 0.5*(a^2 + b^2));
22  C22 = 0.05*(a^2 − b^2);
23  C40 = (15/7)*(C20^2 + 2*C22^2);
24  C42 = (5/7)*C20*C22;
25  C44 = (5/28)*C22^2;
26
27  x = X(1);
28  y = X(2);
29
30  r = sqrt( x^2 + y^2 );
31  r_2 = r^2;
32  r_3 = r^3;
33  r_4 = r^4;
34  x_2 = x^2;
35  x_4 = x^4;
36  y_2 = y^2;
37  y_4 = y^4;
38
39  % Defining terms of the two equations of motion
```

```
40  E1_T1 = Omega^2;
41  E1_T2 = C20/2;
42  E1_T3 = 1*C22*(7*y_2 - 3*x_2)/r_2;
43  E1_T4 = C40/8;
44  E1_T5 = 0.5*C42*(9*y_2 - 5*x_2)/r_2;
45  E1_T6 = 7*C44*(5*x_4 - 46*x_2*y_2 + 21*y_4)/r_4 ;
46
47  E2_T1 = Omega^2;
48  E2_T2 = C20/2;
49  E2_T3 = 1*C22*(3*y_2 - 7*x_2)/r_2;
50  E2_T4 = C40/8;
51  E2_T5 = 0.5*C42*(5*y_2 - 9*x_2)/r_2;
52  E2_T6 = 7*C44*(5*y_4 - 46*x_2*y_2 + 21*x_4)/r_4 ;
53
54  f1 = E1_T1 - ( (1/r_3)*( 1 - (3/r_2)*( E1_T2 + E1_T3 ) +...
55  (15/r_4)*(E1_T4 + E1_T5 + E1_T6) ));
56  f2 = E2_T1 - ( (1/r_3)*( 1 - (3/r_2)*( E2_T2 + E2_T3 ) +...
57  (15/r_4)*(E2_T4 + E2_T5 + E2_T6) ));
58
59  LHS_Eq1_Sqrd = f1^2;
60  LHS_Eq2_Sqrd = f2^2;
61
62  F = max(LHS_Eq1_Sqrd, LHS_Eq2_Sqrd);
63
64  end
```

A.3.3   Determination of Lagrangian Points - L1 and L2

```
1  % Function file for determining Lagrangian Points L1 and L2
2  % for an Ellipsoid
3
4  % The equations of motion are as follows
5  % Omega^2 - [(1/r^3)*{1 - (3/r^2)*[C20/2 + C22*(7*y^2 - 3*x^2)/r^2]..
6  % + (15/r^4)*[ C40/8 + 0.5*C42(9*y^2 - 5*x^2)/r^2 + ...
7  % 7*C44*(5*x^4 -46x^2*y^2 + 21*y^4)/r^2 ]} = 0...eq(1)
8
9  function F = Lagrangian_Points_L123_Ellipsoid(X)
10
11  global Omega
12
13  x = X(1);
14  y = 0;
15
16  r = abs(x);
17  r_2 = r^2;
18  r_3 = r^3;
19  r_4 = r^4;
20  x_2 = x^2;
21  x_4 = x^4;
```

```matlab
22  y_2 = y^2;
23  y_4 = y^4;
24  r_2 = r^2;
25  r_3 = r^3;
26  x_2 = x^2;
27
28  % Special case 1:
29  % a, b and c are non-dimensional a_bar = a/r0
30  b = 2;
31  c = 1;
32  a = 3;
33
34  % C20, C22, C40, C42, C44 are non-dimensional
35  C20 = 0.2*(c^2 - 0.5*(a^2 + b^2));
36  C22 = 0.05*(a^2 - b^2);
37  C40 = (15/7)*(C20^2 + 2*C22^2);
38  C42 = (5/7)*C20*C22;
39  C44 = (5/28)*C22^2;
40
41  %  Special case 2, The ellipsoid becomes a sphere:
42  % b = 1;
43  % c = b;
44  % a = b;
45
46  % Defining terms of the equation of motion
47  E1_T1 = Omega^2;
48  E1_T2 = C20/2;
49  E1_T3 = 1*C22*(7*y_2 - 3*x_2)/r_2;
50  E1_T4 = C40/8;
51  E1_T5 = 0.5*C42*(9*y_2 - 5*x_2)/r_2;
52  E1_T6 = 7*C44*(5*x_4 - 46*x_2*y_2 + 21*y_4)/r_4 ;
53
54  f1 = E1_T1 - ( (1/r_3)*( 1 - (3/r_2)*( E1_T2 + E1_T3 ) +
55  (15/r_4)*(E1_T4 + E1_T5 + E1_T6) ));
56  LHS_Eq1_Sqrd = f1^2;
57
58  F = LHS_Eq1_Sqrd;
59
60  end
```

A.4   Validation

A.4.1   Determination of the Radius and Density of spheres 1 and 3 as a function of the semi-minor axis length b

```matlab
1  % Program to compute radius and density of spheres 1 and 3
2  % as a function of the semi-minor axis length b
3  clc
4  clear all
```

```matlab
close all

for b = 0.01:0.01:0.99;

p = (7./5).*(1-b);
q = 2.*b.*(1-b);
r = ((b.^2).*(1-b)) - ((1./5).*(1+b.^2)) - ((2./5).*(b.^3));

Rs1_1 = (- q + sqrt( q.^2 - 4.*p.*r)) ./ (2.*p);
Rs1_2 = (- q - sqrt( q.^2 - 4.*p.*r)) ./ (2.*p);

figure(1)
plot(b,Rs1_1,'-bo');
axis([0.01 0.99 0 +1])
xlabel('b')
ylabel('Rs_1')
title('Variation of Radius of spheres 1 & 3 as a
function of Radius of sphere 2')
hold on

rho1_1 = (b.^2).*(1-b) ./ (2.*Rs1_1.^3);
rho1_2 = (b.^2).*(1-b) ./ (2.*Rs1_2.^3);
disp(rho1_1);
disp(rho1_2);

figure(2)
plot(b,rho1_1,'-bo');

xlabel('b')
ylabel('\rho_1')
title('Variation of Density of spheres 1 & 3 as a
function of Radius of sphere 2')
hold on

end
```